Dalton Transactions

Mesoporous SBA-15 Modified with Titanocene Complexes and Ionic liquids: Interactions with DNA and other Molecules of Biological Interest Studied by Solid State Electrochemical Techniques

Journal:	*Dalton Transactions*
Manuscript ID	DT-ART-05-2018-002011.R1
Article Type:	Paper
Date Submitted by the Author:	n/a

Complete List of Authors:	del Hierro, Isabel; Universidad Rey Juan Carlos, Biología, Geología, Física y Química Inorgánica Gómez-Ruiz, Santiago; Universidad Rey Juan Carlos, Departamento de Biología y Geología, Física y Química Inorgánica Pérez, Yolanda; Universidad Rey Juan Carlos, Cruz, Paula; Universidad Rey Juan Carlos Prashar, Sanjiv; Universidad Rey Juan Carlos, Química Inorgánica Fajardo, Mariano; Universidad Rey Juan Carlos, Química Inorgánica y Analítica

Dalton Transactions

Guidelines to Referees

Communications & Papers

The international journal for high quality, original research in inorganic and organometallic chemistry

http://www.rsc.org/dalton

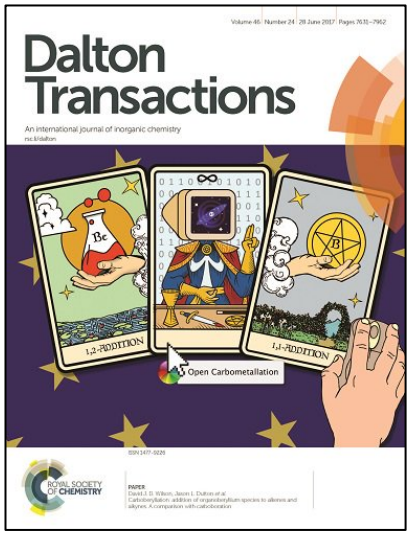

Dalton Transactions wishes to encourage high quality articles reporting exciting new developments in inorganic chemistry.

For an article to be accepted, it must report new, high-quality research and make a significant contribution to the field.

Manuscripts that describe purely physical, crystallographic or computational studies must include the clear relevance of the work to the broad inorganic chemistry readership of *Dalton Transactions*.

Communications must report chemistry of sufficient importance and impact to justify preliminary publication. **Papers** should report more complete studies.

***Dalton Transactions'* Impact Factor is 4.029** (2016 Journal Citation Reports®)

Routine or unnecessarily fragmented work, however competently researched and reported, should not be recommended for publication.

Thank you very much for your assistance in evaluating this manuscript

Dr Andrew Shore (dalton@rsc.org)
Royal Society of Chemistry
Editor, *Dalton Transactions*

Professor John Arnold
University of California, Berkeley
Chair, *Dalton Transactions* Editorial Board

General Guidance (for further details, see the RSC Refereeing Procedure and Policy)

When preparing your report, please:

- Comment on the **originality**, **importance**, **impact** and **scientific reliability** of the work
- State clearly whether you would like to see the paper accepted or rejected and give detailed comments (with references, as appropriate) that will help both the Editor to make a decision on the paper and the authors to improve it

Please inform the Editor if:

- There is a conflict of interest
- There is a significant part of the work which you are not able to referee with confidence
- If the work, or a significant part of the work, has previously been published, including online publication (*e.g.* on a preprint server/open access server)
- You believe the work, or a significant part of the work, is currently submitted elsewhere
- The work represents part of an unduly fragmented investigation

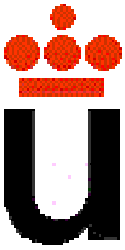

Dr. Isabel del Hierro

Departamento de Biología, Geología, Física y Química Inorgánica

Escuela Superior de Ciencias Experimentales y Tecnología

UNIVERSIDAD REY JUAN CARLOS

C/ Túlipan S/N 28933 Móstoles. Madrid. Spain

Isabel.hierro@urjc.es

Phone 0034 914887022 Fax 0034 914888143

Please find enclosed the manuscript entitled "**Mesoporous SBA-15 Modified with Titanocene Complexes and Ionic liquids: Interactions with DNA and molecules of biological interest studied by solid state electrochemical techniques"** that we wish to publish as a regular full paper in *Dalton Transactions* This article is original and the results are not being considered for publication elsewhere. All co-authors are aware of the submission and agree to its publication in *Dalton Transactions.*

Titanocene dichloride is by far the most studied titanium compound in anticancer chemotherapy, although its use in humans has been discontinued from clinical studies due to solubility problems and lack of activity under physiological conditions. A plausible alternative for this kind of compounds is the use of different scaffolds for the protection of the titanocene derivatives in order to achieve a more effective delivery or cytotoxic action to the cancer cells. Thus, our group has recently studied the use of silica-based nanostructured materials as carrier vehicles of titanocene derivatives and other metallodrugs observing an enhancement in the cytotoxic activity per active metal species and a decrease in the speciation processes and uncontrolled hydrolysis of the supported metal complex.

In this context, we have designed a set of experiments in order to gain insights into the transportation processes and binding behaviour of titanocene dichloride grafted onto mesoporous silica SBA-15. This has been undertaken by mimicking physiological media and studying the interaction of titanocene-functionalized silica-based materials with some molecules of biological interest associated with the cytotoxic action of titanocene derivatives

such as guanosine, nucleic acids, bovine serum albumin and transferrin by means of solid state voltammetry techniques. The present study reveals the high stability of the titanocene-functionalized materials in physiological medium and the very high affinity to transport / serum proteins such as transferrin or albumin. In addition, the electrochemical study indicates a low degree of affinity of titanocene-functionalized materials with DNA chains. This may indicate that the interaction of the materials with DNA is perhaps the limiting step for the degree of cytotoxic action against cancer cells.

With best regards,

Yours sincerely,

Dr. I. del Hierro

Mesoporous SBA-15 Modified with Titanocene Complexes and Ionic liquids: Interactions with DNA and other Molecules of Biological Interest Studied by Solid State Electrochemical Techniques.

Isabel del Hierro*, Santiago Gómez-Ruiz*, Yolanda Pérez, Paula Cruz, Sanjiv Prashar, Mariano Fajardo.

Departamento de Biología y Geología, Física y Química Inorgánica, ESCET, Universidad Rey Juan Carlos. Calle Tulipán S/N, E-28933 Móstoles (Madrid) Spain.

Abstract

Immobilization of two titanocene complexes on SBA-15 has been accomplished following post synthetic procedures. The ionic liquid, 1-methyl-3-[(triethoxysilyl)propyl]imidazolium chloride, has also been incorporated into the titanium containing materials in order to determine its influence in the interaction with molecules of biological interest. Cyclic voltammetry has been used to study the influence of the ionic liquid on the mechanism of reduction of titanocene derivatives. The interaction of titanocene and titanocene / ionic liquid-containing mesoporous silica SBA-15 materials with molecules of biological interest associated with important processes of metallodrug action against cancer cells has been studied. Thus, we have carried out hydrolysis experiments of the materials functionalized with titanocene derivatives in physiologic medium to determine their stability and the interaction with serum / transport proteins such as transferrin and BSA and with target molecules such as guanosine, single stranded DNA and double-stranded DNA by means of solid state voltammetry techniques. A qualitative analysis of the data based on peak current and reduction potential value changes of the couple Ti(IV) / Ti(III) in the presence of biomolecules at physiological pH has revealed that grafted titanocene complexes show higher affinity for serum / transport proteins than for nucleic acids indicating that the transportation steps to cell may be easier than the subsequent attack to DNA.

Keywords: Titanocene, ionic liquids, metal-biomolecule interactions, mesoporous materials, solid-state electrochemistry

Graphical Abstract

SBA-15 has been functionalized by titanocene derivatives and an ionic liquid incorporated in the resulting materials. Electrochemical properties of the prepared materials and their chemical interactions with molecules of biological interest associated with the cytotoxic mechanism of action in cancer cells have been studied by differential pulse and cyclic voltammetry.

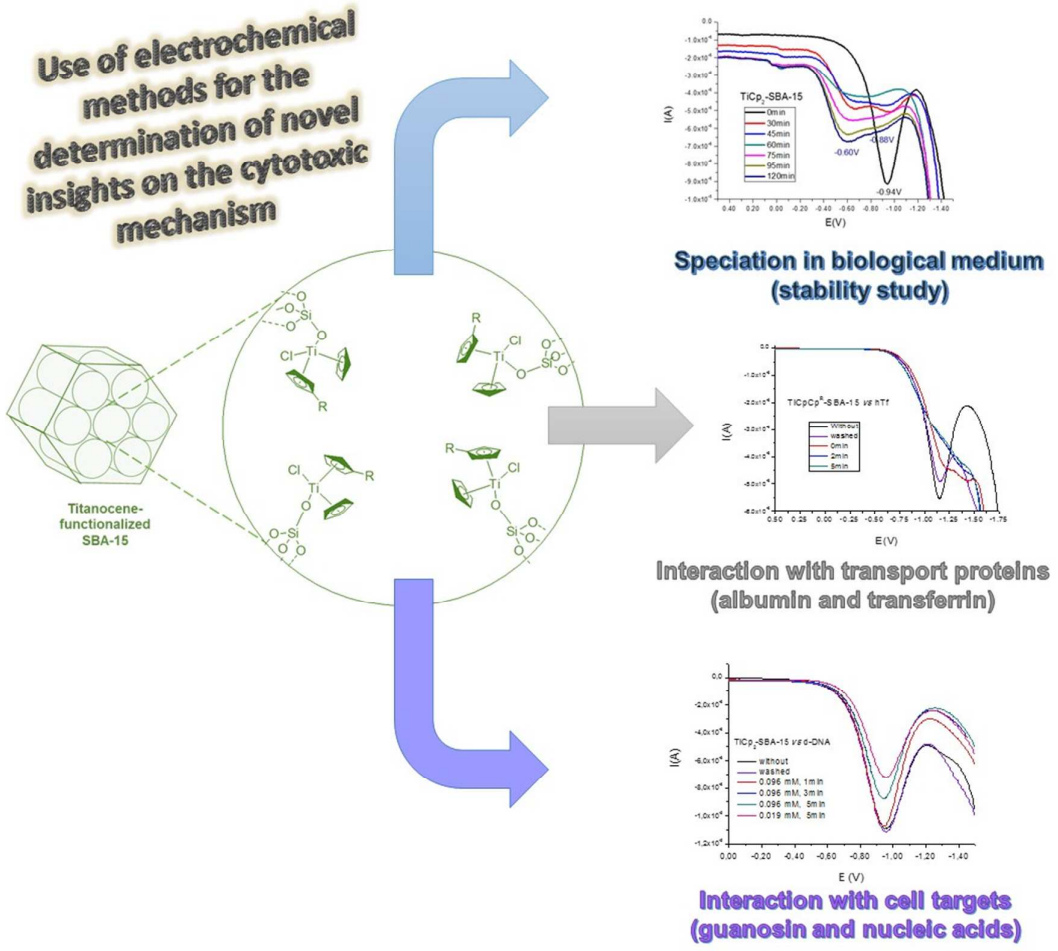

1. Introduction

Metallocene complexes [M (η^5-C_5R_5)$_2$Cl$_2$] (M = Ti, Mo, V, Nb; R = H, alkyl, alkenyl, phenyl, etc.) are an interesting class of compounds which have shown anticancer properties as reported in the initial studies of Köpf-Maier[1] and by other research groups.[2,3] Titanocene dichloride, [Ti(η^5-C_5H_5)$_2$Cl$_2$], is by far the most studied titanium compound in anticancer chemotherapy, although its use in humans has been discontinued from clinical studies due to solubility problems and lack of activity under physiological conditions.[4] However, the search for more active titanocene compounds is ongoing and it is an important research field which hopefully will lead to the application of titanium complexes in new clinical trials.

It is generally agreed that titanocene derivatives may change their structure in the passive or active transportation steps inside the cell or during the membrane crossing processes. [5] Therefore, a plausible alternative for this kind of compounds is the use of different scaffolds for the protection of the titanocene derivatives in order to achieve a more effective delivery or cytotoxic action to the cancer cells.[6,7] Thus, our group has recently studied the use of silica-based nanostructured materials as carrier vehicles of titanocene derivatives and other metallodrugs observing an enhancement in the cytotoxic activity per active metal species and a decrease in the speciation processes and uncontrolled hydrolysis of the supported metal complex. This leads to a higher metal uptake compared to their corresponding non-encapsulated metal-based drug. [8,9,10,11,12,13,14] In addition, silica-based nanostructured systems functionalized with titanocene derivatives usually act as “non-classical” drug-delivery systems as they do not require the release of the metal complex to the physiological medium to be cytotoxic to cancer cells. Indeed, they seem to act as an entire nanoparticulated system with a distinct mechanism of cell death induction.[6,12] Thus, titanocene-functionalized nanostructured materials show different dynamics of apoptotic morphological and functional changes and induce the programmed cell death in tumour cell populations by different methods to that of their corresponding free titanocene derivatives.[12,15]

In spite of the synthetic and cytotoxic advances reported by the scientific community in this field, there is still very little understood about how the encapsulation and use of carrier vehicles for titanocene derivatives promote such big differences in the cytotoxic studies against cancer cell lines. Most of the studies have been based on cytotoxic and release studies in physiological medium but less is known about the changes in the nanomaterials during the *in vitro* tests (possible speciation) and these changes may be crucial to understand the transport processes associated with the interpretation of the cytotoxic properties of the nanostructured materials.

Previous studies from our [16] and other research groups [17] have shown that the use of electrochemical techniques are very useful for the interpretation of the possible interactions of titanocene derivatives with molecules of biological interest in the evaluation of the cytotoxic activity. However, for titanocene-functionalized nanostructured materials much less is known with only a single recent report showing that electrochemical biosensor techniques adopted for the investigation of drug-biomolecule interactions are straight forward and reliable.[18]

In this context, we have designed a set of experiments in order to gain insights into the transportation processes and binding behaviour of titanocene dichloride grafted onto mesoporous silica SBA-15. This has been undertaken by mimicking physiological media and studying the interaction of titanocene-functionalized silica-based materials with some molecules of biological interest associated with the cytotoxic action of titanocene derivatives such as guanosine, nucleic acids, bovine serum albumin and transferrin by means of solid state voltammetry techniques. For comparison purposes a titanocene complex with a monosubstituted alkenyl cyclopentadienyl ligand has also been grafted onto SBA-15 and studied using similar methods and conditions. Furthermore, the titanium-containing nanostructured materials have additionally been functionalized with an ionic liquid (IL). The reason behind this is that ILs have demonstrated their ability to improve the electrochemical response of different nanomaterials [19] It is well known that ILs disperse carbon nanotubes in water and organic solvents [20] having a wide electrochemical window and functioning as agglutinant in the preparation of carbon paste electrodes in analytical sensors. In addition, ILs are able to improve the peak current.[21] Also of interest to the current study is the use of ILs as ligands in the preparation of metallodrugs with anticancer activity.[22]

The present study reveals the high stability of the titanocene-functionalized materials in physiological medium and the very high affinity to transport / serum proteins such as transferrin or albumin. In addition, the electrochemical study indicates a low degree of affinity of titanocene-functionalized materials with DNA chains. This may indicate that the interaction of the materials with DNA is perhaps the limiting step for the degree of cytotoxic action against cancer cells.

2. Results and discussion

2.1. Synthesis and characterization of titanocene-supported materials.

The immobilization of two titanocene compounds, $[Ti(\eta^5\text{-}C_5H_5)_2Cl_2]$ and $[Ti(\eta^5\text{-}C_5H_5)(\eta^5\text{-}C_5H_4R)Cl_2]$ (R = $CMePh(CH_2CH{=}CH_2)$) has been achieved following post synthetic procedures.

The resulting titanium containing materials have been functionalized with the ionic liquid 1-methyl-3-[(triethoxysilyl)propyl]imidazolium chloride (IMIL). Two distinct immobilization procedures have been developed as shown in Scheme 1. Firstly, the material $TiCp_2$-IMIL-SBA-15 was synthesized by grafting the ionic liquid, 1-methyl-3-[(triethoxysilyl)propyl]imidazolium chloride (IMIL) onto previously dehydrated SBA-15, followed by the addition of titanocene to the resulting IMIL-SBA-15 solid. The second procedure involves the preparation of immobilized titanium containing materials $TiCp_2$-SBA-15 and $TiCpCp^R$-SBA-15 in a first step followed by the addition of 1-methyl-3-[(triethoxysilyl)propyl]imidazolium chloride (IMIL) to yield the materials named as IMIL-$TiCp_2$-SBA-15 and IMIL-$TiCpCp^R$-SBA-15.

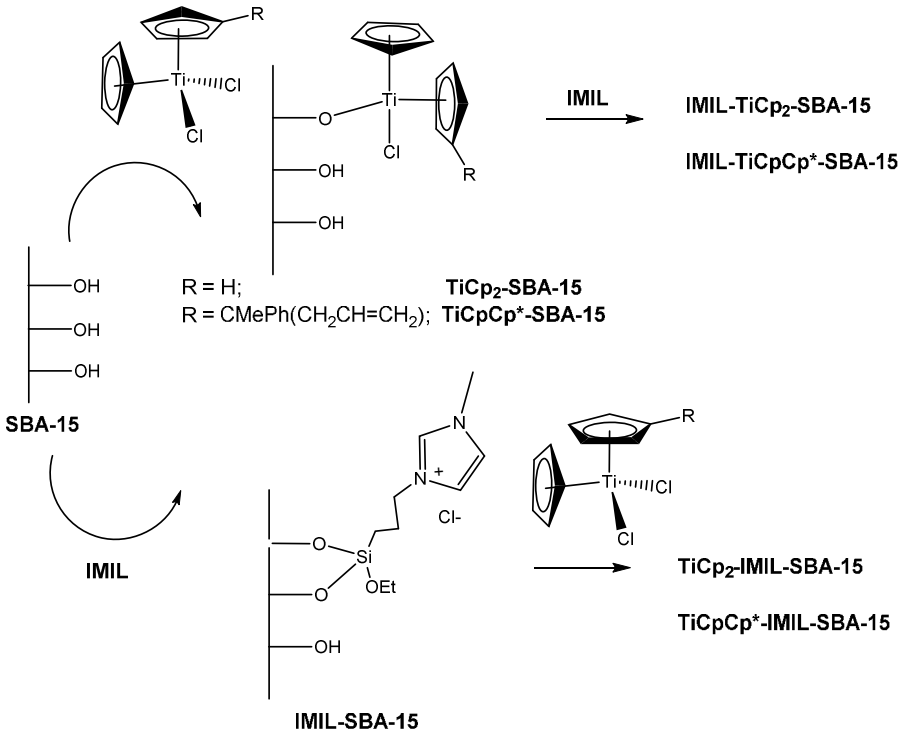

Scheme 1. Preparation of titanocene and IMIL functionalized SBA-15

The crystalline structure of this family of titanium-supported materials was characterized by low-angle XRD (Fig. 1 and Fig S1). The low angle diffraction pattern for pristine SBA-15 shows three reflections at 2θ values of 0.9–2^o, namely, a strong peak (100) and two weak peaks (110) and (200) corresponding to a highly ordered hexagonal mesoporous silica framework as expected for the SBA-15 material. The titanium-containing samples showed similar patterns, indicating that the long-range order of the SBA-15 framework was well retained after the grafting process. In addition, the decrease in the intensity of the (100) diffraction peak at 2θ = 0.95^o upon reaction with the titanium precursor and / or the ionic

liquid, provides evidence of the incorporation of the different fragments which mainly occurs inside the mesoporous channels.

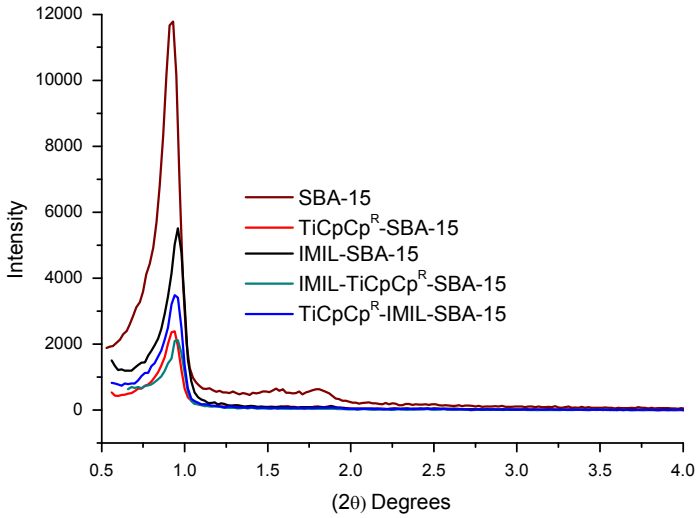

Figure 1. DRX patterns of SBA-15, IMIL-SBA-15, TiCpCp^{R}-SBA-15, IMIL-TiCpCp^{R}-SBA-15 and TiCpCp^{R}-IMIL-SBA-15.

The physical parameters of the synthesized materials such as surface area (S_{BET}), total pore volume and BJH average pore diameter have been measured by nitrogen adsorption experiments. The parent material possesses a S_{BET} of 654 m^2 g^{-1} and a BJH pore diameter of 48 Å. The functionalized materials present a remarkable decrease in the S_{BET} and pore volume in comparison with the parent SBA-15 due to the presence of different fragments anchored to the channels and partially blocking the adsorption of nitrogen molecules (Figure 2 and Table 1).

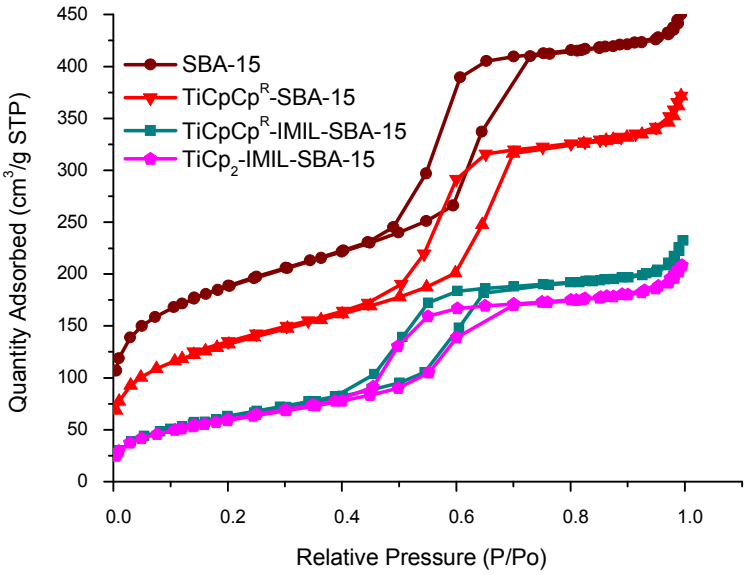

Figure 2. Nitrogen adsorption/desorption isotherms of SBA-15, TiCpCp^R-SBA-15, TiCpCp^R-IMIL-SBA-15 and $TiCp_2$-IMIL-SBA-15 Type IV isotherms typical of mesoporous silica are exhibited.

Table 1. Textural properties of synthesized materials

Material	BET surface area m^2/g	Pore volume, cm^3/g	Pore size, Å	*d*	a_o	Wall thickness Å
SBA-15	654	0.66	49	96.0	110.9	62.1
TiCpCp^R-SBA-15	460	0.53	45	95.0	109.7	64.7
TiCpCp^R-IMIL-SBA-15	215	0.32	56	94.0	108.5	52.5
$TiCp_2$-IMIL-SBA-15	206	0.29	54	94.0	108.5	54.5

Based on the chlorine content obtained by FRX analysis the quantity of molecules attached to the mesoporous silica in IMIL-SBA-15 was calculated to be 0.92 mmol/g (L_o = %Cl×1 / chlorine molecular weight), Taking into account L_0 and S_{BET} of the mesoporous silica, the average surface density of the attached molecules and the average intermolecular distance [23] were calculated as 0.85 (molecules per nm^2) and 1.09 nm, respectively. The amount of titanium and chlorine determined on the basis of XRF measurements for the different materials is shown in Table 2. Certain conclusions can be drawn from this data considering that titanocene derivatives react with the silanol groups available on the silica surface *via*

protonolysis of the Ti-Cl bonds. A comparison between the titanium complexes used as precursor shows that steric requirements is a relevant factor. Thus, the grafting efficiency for the larger $TiCpCp^R$-SBA-15 is nearly three times lower than that of $TiCp_2$-SBA-15, In both materials the amount of chlorine suggests the reaction of the titanocene precursor proceeds *via* one chlorine atom giving evidence for the coordination of titanium in a tetrahedral environment with two Cp ligands, a chlorine atom and one of the oxygens of a silanol group of the silica surface acting as the formal fourth ligand, via formation of a Si-O-Ti bond (Scheme 1). Furthermore, in the case of the subsequent functionalization of the titanocene containing materials with IMIL, the amount of ionic liquid grafted is low, presumably due to the saturation of the surface. The ratio IMIL / Ti estimated on the basis of these data (excluding the chlorine percentage due to Ti-Cl unit) clearly depends on the material and the degree of saturation of the parent silica. Therefore, the ratio increases when the amount of grafted titanium complex decreases.

Table 2. FRX data of the synthesized materials

Material	**FRX**			
	%Ti	mmol/g	%Cl	mmol/g
IMIL-SBA-15			3.27	0.92
$TiCp_2$-SBA-15	1.48	0.31	0.90	0.25
$TiCpCp^R$-SBA-15	0.53	0.11	0.41	0.12
IMIL-$TiCp_2$-SBA-15	1.35	0.28	2.45	0.69
IMIL-$TiCpCp^R$ -SBA-15	0.55	0.12	3.16	0.89
$TiCp_2$-IMIL-SBA-15	0.60	0.13	4.61	1.30

All the synthesized materials have also been characterized by FT-IR spectroscopy. A comparison between the FT-IR spectra of the pristine SBA-15 and the hybrid-SBA-15 materials is shown in Figures 3 and S2. After IMIL immobilization the bands due to the ν(C–H) stretching vibrations appeared at 2967, 2940 and 2888 cm^{-1}; and the band attributed to the C=C stretching of the imidazolium group were observed at 1567 cm^{-1}. After chemical immobilization of $TiCp_2Cl_2$ or $TiCpCp^RCl_2$ onto SBA-15 the characteristic weak bands for ν(C–H) stretching vibrations due to cyclopentadienyl rings appeared in the range 2970–2840 cm^{-1}. In addition, bands at ca, 1600 cm^{-1}, expected for the cyclopentadienyl ligands, overlapped with that of the physisorbed water bands. These data indicate that the functionalization of the surface with the corresponding IMIL and titanocene compounds has taken place.

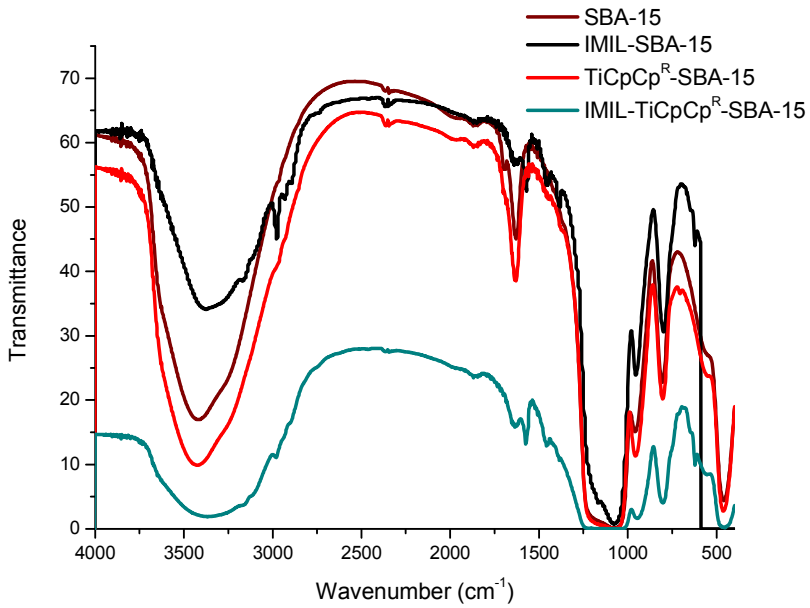

Figure 3. FTIR spectra of SBA-15, IMIL-SBA-15, TiCpCp^R-SBA-15 and IMIL-TiCpCp^R-SBA-15.

The ^{13}C CP MAS NMR spectra of TiCpCp^R-SBA-15, IMIL-SBA-15 and TiCpCp^R-IMIL-SBA-15 are shown in Figure 4. The spectrum of grafted substituted titanocene, TiCpCp^R-SBA-15, showed a set of signals in the range between 120-129 ppm attributed to the unsubstituted and monosubstituted cyclopentadienyl rings and the phenyl substituent. The intense signals observed at 68 and 25 ppm, correspond to THF used in the synthesis procedure. The resonances due to the carbon atoms of the alkenyl substituent were poorly defined at 29, 44 and 111 ppm, The ^{13}C PDA MAS NMR spectrum of IMIL-SBA-15 material showed signals at 9, 22 and 50 ppm corresponding to the carbon atoms of the propyl chain -Si-*C*H$_2$-, -CH$_2$-*C*H$_2$-CH$_2$- and -CH$_2$-*C*H$_2$-*C*H$_2$-N, respectively. The peaks due to the carbons of the heterocycle appeared at 135 ppm (N-*C*-N) and at 121 ppm (N-*C*H-*C*H-N) and the peak attributed to the methyl imidazolium group appeared at 34 ppm. In addition, two signals were observed at 14 and 55 ppm attributed, respectively, to the methyl and methylene groups of unreacted ethoxy units (*C*H$_3$*C*H$_2$O)Si of the silylating agent.

In the spectrum of TiCpCp^R-IMIL-SBA-15, apart from the peaks assigned to the IMIL ligand (similar to those of IMIL-SBA-15), additional peaks corresponding to the titanocene compound were observed. However, some of the resonances of the cyclopentadienyl rings were partially overlapped with those of the tethered IMIL moiety. In addition, the signals corresponding to the supported titanocene appeared in the spectrum although clearly deshielded in comparison with the signals found in the spectrum of TiCpCp^R-SBA-15.

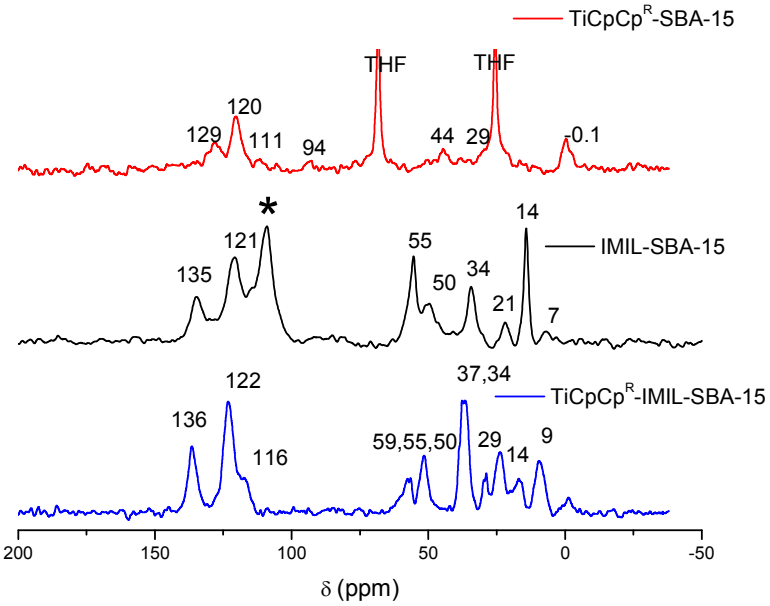

Figure 4. ^{13}C CP NMR Spectra of TiCpCp^{R}-SBA-15, TiCpCp^{R}-IMIL-SBA-15 and IMIL-SBA-15, *Rotor signal.

DRUV-Vis spectra of the studied materials were also recorded (Figure 5). The titanocene functionalized materials $TiCp_2$-SBA-15 and TiCpCp^{R}-SBA-15 displayed a diffuse reflectance spectrum composed of three different signals located at 214 and shoulders at 250 and 330 nm. The first signal has been assigned to the electronic transitions caused by the Ti-O bonds, while the other two have been attributed to the coordination of the cyclopentadienyl rings to the metal. The bathochromic shift of the band at ca 250 nm suggests a decrease in the electronic density around titanium after functionalization. On the other hand, when the material was treated with the ionic liquid, the DRUV spectrum slightly changed. The spectrum of TiCpCp^{R}-IMIL-SBA-15 showed one strong signal around 215 nm associated with the Ti-O bond. The intensity of the signals due to the cyclopentadienyl ligands decreased and shifted to lower wavelengths compared with TiCpCp^{R}-SBA-15, suggesting a strong influence of the IMIL ligands on the environment of the titanium atom bonded to the silica surface.

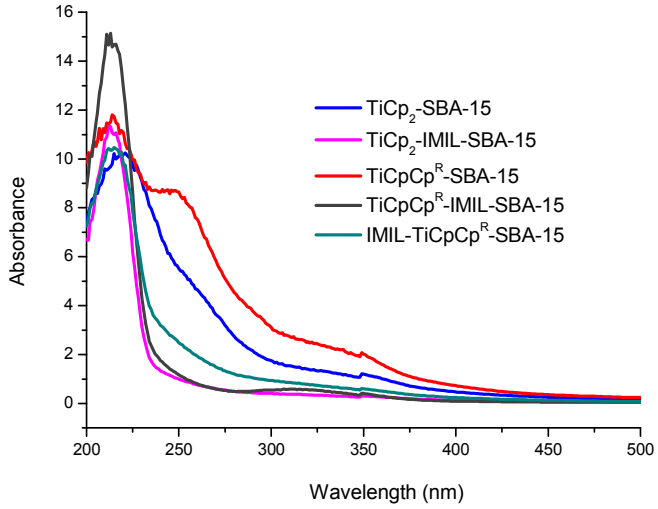

Figure 5. DRUV-Vis Spectra of $TiCp_2$-SBA-15, $TiCpCp^R$-SBA-15, $TiCp_2$-IMIL-SBA-15, $TiCpCp^R$-IMIL-SBA-15 and IMIL-$TiCpCp^R$-SBA-15.

2.2. Electrochemical Studies

2.2.1. Electrochemical characterization of titanocene compounds in THF solution with ILs as co-solvent

To study the influence of the ILs on the electronic structure of the titanocene derivatives, UV-vis spectra and cyclic voltammograms were recorded in organic solvents (Figure S3). It is important to note that the electronic spectra of the titanocene derivatives in dichloromethane showed a strong band around 260 nm attributed to low-energy transitions of the LMCT type in these pseudo-tetrahedral complexes involving the promotion of an electron from the Cp^- or Cl^- ligands to the d^0 metal centre and a weak band around 400 nm assigned to the cyclopentadienyl ligands. For both compounds, no changes were observed in the position or intensity of the strong band attributed to the LMCT after ionic liquid addition to the solution. However, the intensity of the band around 400 nm in the non-substituted titanocene ($TiCp_2Cl_2$) spectrum decreased significantly, supporting a clear interaction between titanocene derivatives and the ILs.[24] This interaction was not observed in the case of substituted titanocene ($TiCpCp^RCl_2$) probably due to greater sterical requirements imposed by the bulky substituent. The interaction of titanocene derivatives with IMIL was also studied by monitoring the changes of the cyclic voltammograms of the complexes upon addition of the ILs. The mechanism for the electrochemical reduction of titanocene $TiCp_2Cl_2$ in donor solvents was first described by Laviron et al. [25] The most characteristic feature of the cyclic voltammogram of titanocene is the wave of the redox couple $[TiCp_2Cl_2]/[TiCp_2Cl_2]^-$ (Figure S4). The original

proposal of Laviron was the existence of an E_qC_i mechanism where the *quasi* reversible electrochemical reduction of $[TiCp_2Cl_2]$ is followed by the fast and chemically reversible cleavage of the anion $[TiCp_2Cl_2]^-$. More detailed studies carried out by different groups, for example Daasbjerg et al,[26] showed additional small oxidation waves while examining the influence of concentration and scan rate. These additional signals have been attributed to the oxidation processes of $[TiCp_2Cl]$ and the dimer $[\{TiCp_2Cl\}_2]$ formed *in situ*.

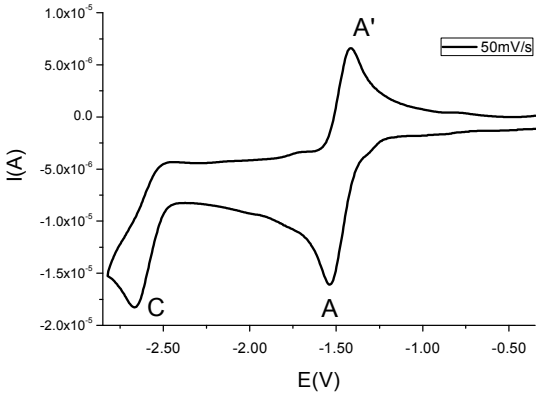

Figure 6. Cyclic voltammogram of $TiCpCp^RCl_2$ scan rate 50 mV/s in THF as solvent, Bu_4NPF_6 as electrolyte (0.2M), GC as working electrode, Pt as counter electrode and Fc/Fc^+ as internal standard (Fc = $[Fe(\eta^5\text{-}C_5H_5)]$).

In cyclic-sweep voltammogram of $TiCpCp^RCl_2$, two prominent electrochemical reduction processes were apparent (See Figure 6 and Scheme 2). In a THF solution, a reduction peak at $E_{1/2}(A/A') = -1.36$ V was observed, which can be assigned to the first electron uptake by $[TiCpCp^RCl_2]$. A decrease in the peak current ratio $I_{ox}(A')/I_{red}(A)$ with increasing sweep rate is in agreement with the dichloride anion formation and a rapid and reversibly dissociation to give a neutral, solvated monochloride complex. Its oxidation occurs after uptake of Cl^- (i,e, regeneration of the dichloride anion), at peak A' or at peak B' (peak not seen). The latter process, labelled as B', would generate the solvated cation $[TiCpCp^RCl(THF)]^+$. The reduction process at $E_{red}(C) = -2.66$ V, which can be assigned to a second one-electron reduction, namely, $[TiCpCp^RCl(THF)] + e^- \rightarrow [TiCpCp^RCl(THF)]^-$, does not have an associated re-oxidation peak. This lack of re-oxidation peak indicates the chemical decay of the Ti(II) species formed. The process is controlled by diffusion as it is demonstrated in the linear plot of $I_{red}(A)$ vs, square root of scan rate through the origin ($I = -8\cdot10^{-8}\text{-}1\cdot10^{-6}\nu^{1/2}$, $R^2 = 0.9901$) (Figure S5).

A cyclic voltammetry study using THF as solvent and the ionic liquid 1-methyl-3-[(triethoxysilyl)propyl]imidazolium chloride (IMIL) as co-solvent shows different behaviour for

the unsubstituted ($TiCp_2Cl_2$) and the monosubstituted ($TiCpCp^RCl_2$) titanocene complexes. Firstly, for comparison purposes, the electrochemical behaviour of IMIL was studied in a THF solution, obtaining a silent voltammogram over a wide range of potential values. At higher potential values an increase of the cathodic current takes place probably due to the monoelectronic reduction of the imidazolium cation [27] (See Figure S6). The cyclic voltammogram of $[TiCpCp^RCl_2]$ recorded under these experimental conditions showed the same reduction peak A at E_{red} (A) = -1.36 V (Figure 7). However, in contrast with that observed in THF, the reduction stage was irreversible. At slow sweep rates the system A/A' was observed. Nevertheless, when the scan rate was increased, two anodic peaks A' and B' at E_{ox}(B') = -0.90 V were obtained. In addition, peak A' decreased and peak B' increased until at high sweep rates only B' practically appeared. As previously published, the addition of an electron donating co-solvent shifts the equilibrium $[TiCpCp^RCl_2] + e^- \leftrightarrows [TiCpCp^RCl_2]^-$ to the right due to its coordination to the titanium centre.[28] $[TiCpCp^RCl_2]^-$ oxidation wave decreased at the expense of a new wave at a higher potential value (less negative) assigned to the new $[TiCpCp^RCl(L)]$ solvent coordinated species. Peak B' can be seen to be due to the reaction $[TiCpCp^RCl(L)] \leftrightarrows [TiCpCp^RCl(L)]^+ + e^-$. For these species the reaction proceeds to the species $[TiCpCp^RCl(L)]$, without any dependence on solvent. The electron uptake is followed by the ligand exchange - Cl^- / + L, where L is the solvent or the electrodonating IMIL (through the imidazolium unit) (See Scheme 2). For comparative purposes, the cyclic voltammogram of the unsubstituted titanocene was also recorded offering similar conclusions (See Figure S7).

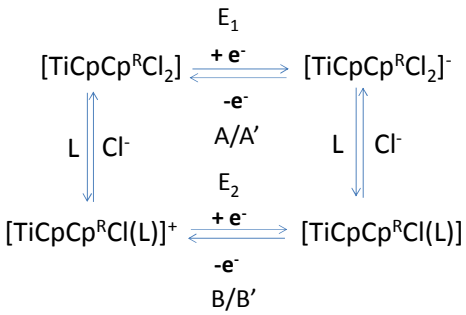

L = THF, IMIL

Scheme 2. Proposed redox mechanism for $[TiCpCp^RCl_2]$ in the presence of THF and THF and ionic liquid, 1-methyl-3-[(triethoxysilyl)propyl]imidazolium chloride.

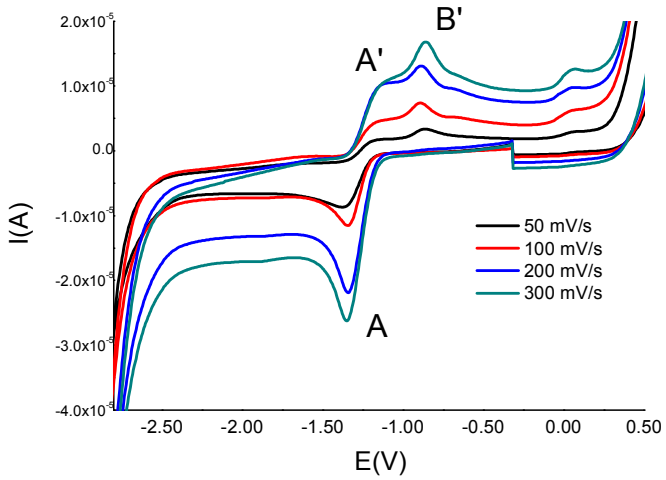

Figure 7. Cyclic voltammogram of $TiCpCp^RCl_2$ with IMIL as co solvent, scan rate from 50-100 mV/s, from scan 1-10, in THF as solvent, Bu_4NPF_6 as electrolyte (0.2 M), GC as working electrode, Pt as counter electrode and Fc/Fc^+ as internal standard.

Table 3 shows the $E_{1/2}$ potentials in THF and cathodic potential with IMIL as co-solvent for the redox couple Ti(IV)/Ti(III) (A/A') of the titanocene complexes. As can be observed, IMIL gave an increased negative reduction potential; 260 mV for $[TiCp_2Cl_2]$ and 130 mV for $[TiCpCp^RCl_2]$. These results are in agreement with those obtained by UV-studies. The presence of the bulky substituent has a notable effect on the interaction of the titanocene complex with IMIL, being based due more to steric requirements than electronic effects, as demonstrated by the similar potential reductions observed for the two titanium complexes (See Table 3).

Table 3. $E_{1/2}$ potentials in THF/ Bu_4NPF_6 and cathodic potential with IMIL as co solvent for the redox couple Ti(IV)/Ti(III) of the titanocene complexes.

Complex	$E_{1/2}$ (V)
$TiCp_2Cl_2$	-1.37
$TiCpCp^RCl_2$	-1.36
	E_{red} (V)
$TiCp_2Cl_2$ + IMIL	-1.63
$TiCpCp^RCl_2$ + IMIL	-1.49

2.3. Study of the interaction of titanocene-functionalized materials with biomolecules by solid state voltammetry

To evaluate the therapeutic action of a metallodrug or of nanostructured systems containing metallodrugs, a complete study of the behaviour of the drugs during different phases of their action is required. First, the stability of the compounds or materials in physiologic media, the possilibity of speciation and formation of active or inactive species which may have influence on the final therapeutic effect of the drugs need to be determined, In this context, studies based on hydrolysis, reactions with different ions or the simple observation of their evolution in physiologic conditions are usually need to be carried out in order to determine the stability of the systems.

In addition, transportation processes are crucial in determining the action of a metallodrug or its functionalized nanostructured system. Thus, in the case of titanocene derivatives, in addition to the passive transportation processes due to the intrinsic permeation of the cells, two different mechanisms of active transportation inside the cells are usually agreed upon. These mechanisms are based on the interaction with transport proteins such as human transferrin (hTf), which does not differenciate between titanium and iron and is able to introduce the Ti-containing species inside the cell [29] or albumin (recently shown to be able to introduce titanium ions inside the cells).[30] Finally, the behaviour of the metallodrugs or their functionalized materials with the expected biological target needs to be examined. In the case of titanocene complexes, one of the possible targets is DNA and, therefore, the interaction with nitrogenated bases, nucleosides, nucleotides and DNA chains usually gives clear information about the binding ability and, therefore, affinity towards the biological target.

In this context, since the discovery of the electrochemical activity of nucleic acids by Palecek,[31] interaction with DNA of anticancer drugs and/or other DNA targeted molecules has been the focus of many electrochemical studies. The interaction mechanism can be studied in three different ways, namely, drug modified electrodes, biomolecule modified electrodes and interaction in solution.[32] For interactions in solution, the drug and DNA are placed in the same solution and changes in the electrochemical signals are compared to those of the drug and the free DNA. [33] Osella and coworkers[34] have used cyclic voltammetry to study the binding of titanocene to DNA and transport proteins such as albumin. The binding behaviour has been described throughout by the variations of the reduction peak Ti(IV)/Ti(III) in water/ethanol solutions at different pH values and this has demonstrated that titanocene has a higher affinity for proteins than for nucleis acids. Crumblins et al.[35] have also predicted the Ti_2-hTf reduction potential by comparing redox potentials of Fe(III) and Ti(IV) complexes that mimic the active

site of transferrin, concluding that the redox potential of titanium-hTf is not accesible for biological reducing agents. Li and coworkers [36] have used cyclic voltammetry to determine the reduction potential of titanocene-hTf complex, since this value is relevant to the stability of the complex. The use of polyethyleneamine to prepare a film electrode made possible the measurement of the reduction potential of the complex Ti(IV)-hTf to Ti(III)-hTf, one electron transfer with one proton concomitant per electron, with a more positive reduction potential than that predicted. It has generally been agreed upon that the complex is trapped in a film material, which is similar to the situation *in vivo*, implying that the reduction and release of titanium from hTf is accessible under physiological conditions.

Traditionally, research of surface modified electrodes has involved the study of the electrochemistry of the attached molecules, catalysis and inhibition of various electrochemical processes and applications such as photoelectrodes or analytical determinations. [17,37,38,39] An example is the study of drug-modified electrodes is the by differential pulse voltammetry of the interaction of platinum complexes with DNA at wax impregnated graphite electrode coated with linearized plasmid DNA.[40] The sensor monitors changes in the electro-oxidation response of the surface-confined DNA resulting from its interaction with platinum compounds and requires no label or indicator. The entrapment of double stranded-DNA (d-DNA) into polypyrrole-polyvinyl sulfonate film over indium-tin-oxide (ITO) coated glass has been used as a sensor to detect titanium and platinum drugs at millimolar concentrations by monitoring the decrease of the guanine oxidation signal as a consequence of DNA damage.[38]

Taking into account the previous studies on this topic, in this section, electrochemical biosensor techniques have been employed in the investigation of drug-biomolecule interactions, Cyclic voltammetry (CV) and Differential Pulse Voltammetry (DPV) measurements have been performed to study the electrochemical response of redox-titanium moieties covalently bound to the walls of mesoporous silica SBA-15.[41] The experiments have been carried out at room temperature, using a three-electrode-single compartment electrochemical cell comprising of a modified carbon paste as working electrode, an Ag/AgCl/KCl 3 M reference electrode and a platinum rod counter electrode. A modified carbon paste with titanium immobilized materials has been used as working electrode.

2.3.1. Study of the speciation in physiological medium

It is well known that titanocene [$TiCp_2Cl_2$] undergoes hydrolysis when it is dissolved in water with the loss of the first chloride ligand. The loss of this ligand proceeds too rapidly to be measured, hydrolysis continues under physiological conditions at pH = 7.4 to give the

dihydroxyl titanocene complex [$TiCp_2(OH)_2$] as the predominant species. In addition to the chloride ligands, the Cp rings can also undergo hydrolysis. The result is a complex series of equilibria involving hydrolysed cationic titanocene derivatives resulting in the formation of aqua, hydroxo, μ-hydroxo and μ-oxo species depending on pH, concentration and chloride concentration of the solution. The complete hydrolysis leads to the formation of insoluble titanocene hydrolysis products of empirical formula $TiCp_{0.31}O_{3.0}(OH)$ in 2h after adjusting pH to 7.4. [42,43,44] To begin our electrochemical studies, it is necessary to examine the behaviour of these materials under physiological conditions in order to properly understand their interaction with molecules of biological interest in this media.

In the differential pulse voltammogram (DPV) recorded for $TiCp_2$-SBA-15 immediately after immersion of the graphite/silica working electrode into aqueous phosphate buffer pH 7.4 solution used as electrolyte, appeared a peak in the cathodic scan at –0.95 V. After a very short period of time the DPV evolved; current intensity of the peak at -0.95 V decreased and two new reduction peaks appeared at -0.88 and -0.60 V. In addition, a weak signal appeared at -0.05V (Figure 8). The intensity and wave profile of the cathodic peaks are time dependent, the intensity of the lowest potential peak decreased whilst those at highest potential increased. These signals were still present after 2 hours contact of the electrode and the aqueous media. In a similar experiment using $TiCpCp^R$-SBA-15, the differential pulse voltammogram shows, immediately after immersion in the physiological medium, a peak at -0.89 V whose intensity decreased gradually with time (Figure 9). However, in this case, new signals were not observed at higher potential values. When the DPV was recorded immediately after immersion of the electrode into the aqueous solution at different values of modulation amplitude, the peak current varied, which supports the unambiguous assignation of the reduction process to the titanium electroactive species grafted onto the silica surface (See Figure S8). In addition, no peaks were observed with a pure SBA-15 modified carbon paste electrode; confirming that the peaks had correctly been assigned to the redox system Ti(IV)/Ti(III), demonstrating that titanium was readily accessible to electron transfer reactions in aqueous medium. To discard the existence of Ti-leaching phenomenon which could justify the signals measured by the presence of titanium species in solution, the electrode remained in physiologic medium for an additional 24 hours and new measurements were carried out by using a fresh electrolyte. The voltammogram measured after this time was exactly the same to that obtained at 120 min, In addition, in order to confirm a lack of leaching, DPV and CV of the electrolyte used in the experiments were repeated using a commercial glassy carbon electrode obtaining silent voltammograms in the range under study (See Figure S9). These results support that the

observed electrochemical behaviour is due to titanium moieties covalently attached to the walls of the mesoporous silica particles. In Figure 10A, the cyclic voltammogram of the $TiCp_2$-SBA-15 material recorded 45 minutes after immersion of the fresh smooth electrode surface into the electrolyte solution, is shown. In this voltammogram at least two reduction peaks were observed at -0.95 and -0.60 V, without the presence of anodic waves associated to them. Under identical experimental conditions, the cyclic voltammogram of the $TiCpCp^R$-SBA-15 showed a well-defined reduction peak at -0.95 V with an associated re-oxidation peak in the reverse scan (Figure 10B). There is a linear correlation between current intensity of the couple and square root of scan rate, showing that the kinetics of the overall process was controlled by diffusion behaviour, This corresponds most probably to the pseudo-diffusion of electrons between two adjacent electroactive centres (as titanium atoms are firmly attached to the silica walls of the porous materials), and to counter ion diffusion since the reduction process of titanium requires charge balance by electrolyte cation.[45,46,47]

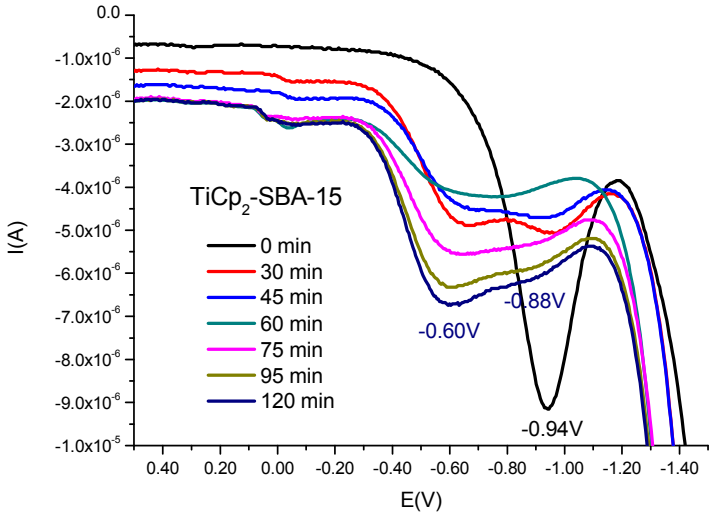

Figure 8. DPV (75 mV modulation amplitude) of $TiCp_2$-SBA-15 immediately after immersion in aqueous phosphate buffer pH 7.4 as electrolyte and at different times vs Ag/AgCl/KCl (3 M) as reference electrode.

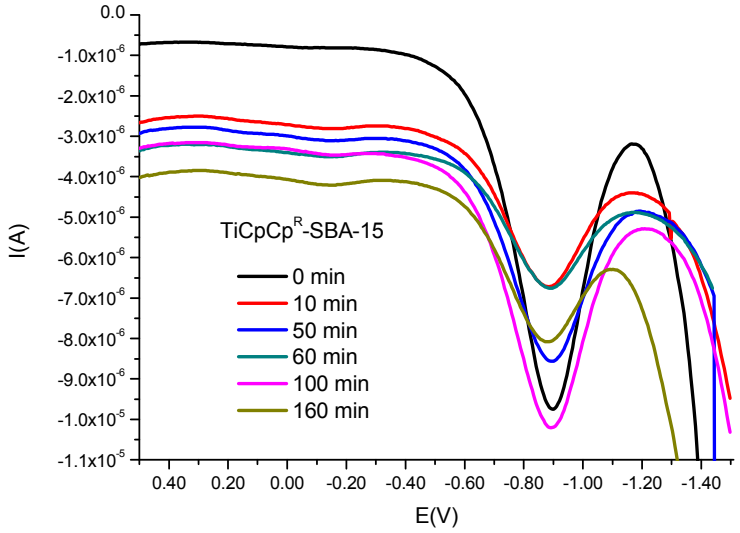

Figure 9. DPV (75 mV modulation amplitude) of TiCpCp^R-SBA-15 at different times after immersion in aqueous phosphate buffer pH 7.4 as electrolyte vs Ag/AgCl/KCl (3 M) as reference electrode.

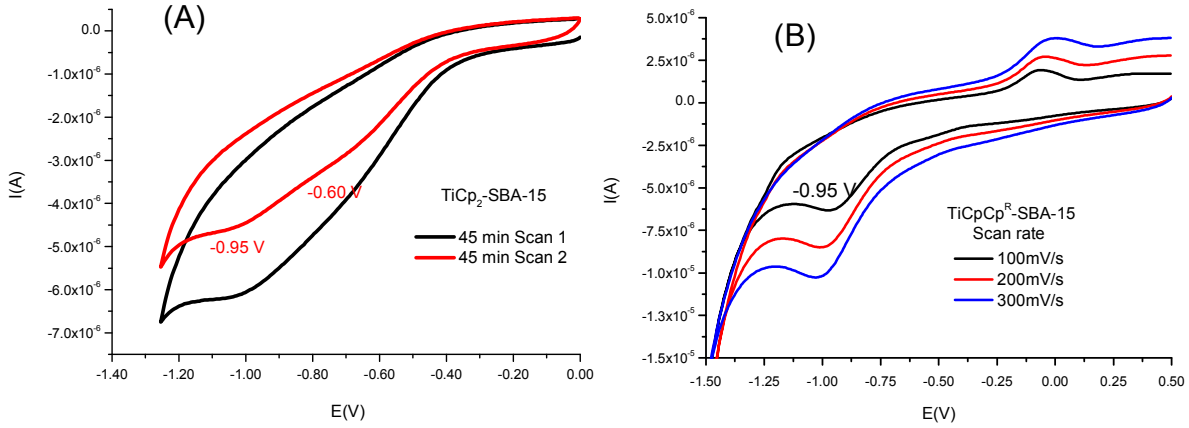

Figure 10. CV of (A) $TiCp_2$-SBA-15 45 min after immersion in aqueous phosphate buffer pH 7.4 as electrolyte (scan 1 and scan 2 at 50 mV/s scan rate) (B) TiCpCp^R-SBA-15 45min after immersion in aqueous phosphate buffer pH 7.4 as electrolyte (scan rate from 100-300 mV) vs Ag/AgCl/KCl (3 M) as reference electrode.

Under these experimental conditions, it seems that four-coordinated species such as "$TiClCp_2$-OSi" are converted into cationic complexes after the hydrolysis of the chloride in a very fast initial step. The peak observed at -0.95 V was assigned to the reduction process

Ti(IV)/Ti(III) of tetra-coordinated titanium centres. By analogy with titanocene compound behaviour in solution, the new peaks at higher potential values (less negative) are probably due to the formation of a different structural titanium species that is more easily reduced as demonstrated by the increase of the potential value (from -0.95 to -0.88 and -0.60 V). A similar pattern has been observed when recording the electrochemical behaviour of titanocene immobilized on mesoporous microspheres by reaction with a grafted triazole ligand with pendant hydroxyl moieties. This triazol-coordinated titanium(IV) complex with an alkoxo and two cyclopentadienyl ligands possesses an extra donor contribution from the N embedded in the triazole ring and initially renders a reduction peak at -1.06 V. As expected, the penta-coordinated titanium derivative is more difficult to reduce than the tetrahedral coordinated species. [18] Similarly, one can hypothesize the formation of cationic species of the type $[TiCp_2(OSi\equiv)]^+$ followed by the formation of $[TiCp_2(OH)(OSi\equiv)]$ [48] (See Scheme 3). On the contrary, the DPV of the substituted grafted titanocene does not show any new signals in the same time interval suggesting its higher stability in comparison with the unsubstituted titanocene complex. The presence of the bulky substituent attached to the cyclopentadienyl ligands may provide a higher stability against the hydrolysis process. In addition, if one accepts the formation of a cationic species, the alkenyl functionality available may cause an intramolecular coordination.[16] This fact and the confinement effect due to the incorporation of the complex into the mesopores, increases the stability of titanium cyclopentadienyl cation against hydrolysis and decomposition.[49]

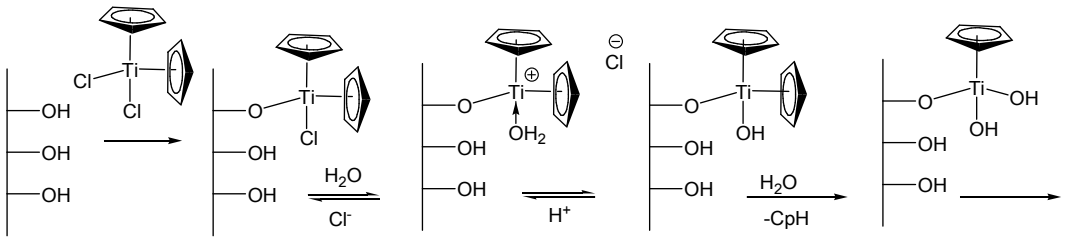

Scheme 3. Hydrolysis mechanism proposal for grafted titanocene complexes onto SBA-15

It has also been reported that, in addition to the hydrolysis of the chloride ligands, the cyclopentadienyl rings can also suffer hydrolysis.[50] Thus, grafted titanocene may react with water to produce a hydroxyl titanium species and free cyclopentadiene. The complete hydrolysis of the tethered titanium complexes would render oxo- and hydroxo-species akin to that previously observed at long time periods.[51] In this present study, longer periods were not examined due to the loss of the mechanical properties of the carbon paste electrode. The hydration of the carbon paste with time means its reutilization is not possible and therefore,

satisfactory measurements of electrochemical properties cannot be achieved. In addition, in some of the measurements at long time periods, the noise, low current peaks and high capacity current observed may also be due to this phenomenon.

Nevertheless, with these studies, we have observed a high degree of stability of the material grafted with the substituted titanocene $TiCpCp^R$-SBA-15 which is higher than that of the material functionalized with the unsubstituted titanocene complex $TiCp_2$-SBA-15. This indicates that $TiCpCp^R$-SBA-15 reacts to a lesser extent with the physiological medium compared to $TiCp_2$-SBA-15. Therefore, it seems clear that the material with the substituted titanocene complex does not easily undergo uncontrolled hydrolysis causing a decrease in speciation processes and formation of unidentified species which might not be cytotoxic. This makes it a promising candidate for therapeutic treatment.

2.3.2. Study of the interaction with transport proteins, albumin and transferrin

The interaction with proteins such as albumin or transferrin is one of the key steps associated with the mechanism of cytotoxic action of titanocene derivatives with the Cp rings in the coordination sphere of the metal playing an essential role. Sadler and co-workers have shown *in vitro*, that both Cp ligands in titanocene are displaced and titanium (IV) is taken up by the vacant iron (III) binding sites in transferrin at blood plasma pH values [29]. Additionally, in release studies, a lowering of pH below 4.5 was necessary to force the coordinated metal to dissociate from the protein.[52] One possible role of the Cp rings is to create a hydrophobic environment for the metal, thus facilitating membrane transport prior to the release of the active species. Upon the uptake of titanocene by transferrin (hTF) into iron specific sites, Cp and Cl ligands must be released to form Ti_2-(hTF) adducts. These results imply that a labile Cp-Ti bond is essential for generating the Ti(IV) active species that are able to reach the cells when titanocene is administered. The solvolysis of the Cp ring represents an important event that must occur slowly enough to allow uptake of titanium species by transferrin and presumably also by albumin. To evaluate the behaviour of materials against serum proteins such as albumin, bovine serum albumin (BSA) has been chosen as a suitable model, due to its structural similarity with human serum albumin (HAS). In BSA interaction and binding certain studies have suggested that metal complexes most likely affect the Trp134 residue found on the surface of the protein and are thus more accessible. In addition, one of the most important properties of albumins is their ability to bind to many different compounds in a reversible manner, often increasing the apparent solubility of hydrophobic drugs in the plasma which influences the circulation, metabolism and efficacy of drugs. [53]

In order to gather additional information about the interaction of the above synthesized materials with transport proteins, an interaction study was conducted in the presence of BSA or h-Tf. Figure 11 shows the DP and CV voltammograms of $TiCp_2$-SBA-15 in the presence of a BSA solution of concentration 4.6 and 9.2 µM in buffer phosphate used as electrolyte. As can be seen, a decrease in the peak current height was observed in DPV in the presence of BSA, this decrease in the height was more pronounced at the highest concentration of BSA; nevertheless, the % interaction calculated for $TiCp_2$-SBA-15 and BSA on the basis of peak current change does shows no dependence on the concentration values (23.9 % for BSA 9.2 µM and 20.1 % for 4.2 µM).[54]

$$\%Interaction = \frac{I_{complex-drug} - I_{complex}}{I_{complex}} \times 100 \qquad \text{(Eq. 1)}$$

An important shift of the potential value was observed from -0.95V to -1.06 V which indicates the formation of a stable adduct or species; in addition, CV confirmed the DPV results. When the electrode surface was thoroughly washed with ultrapure water and a new measurement recorded in pure buffer phosphate, the signal attributed to the initial titanium species was recovered practically unaltered.

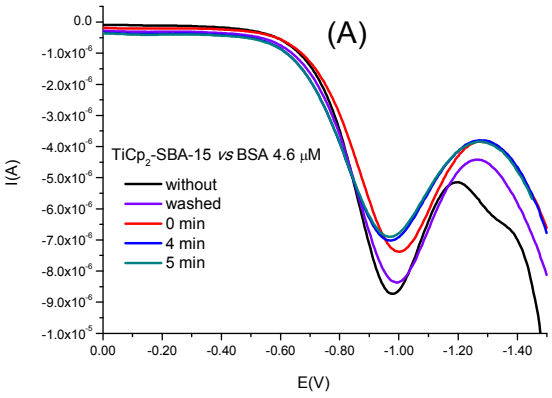

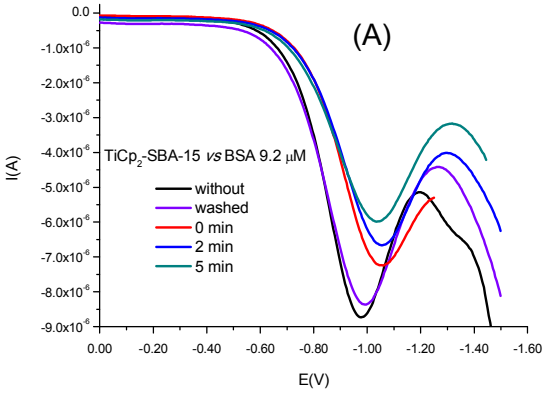

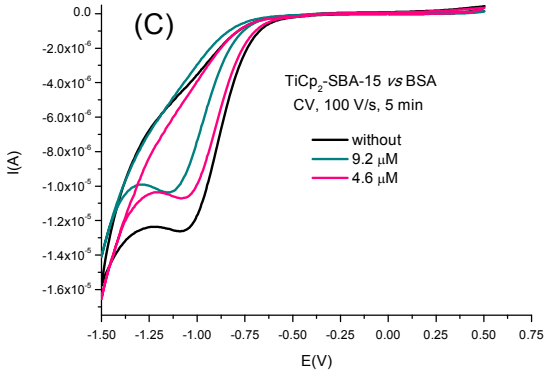

Figure 11. DPV (75 mV modulation amplitude) of $TiCp_2$-SBA-15 /graphite electrode 5 min after immersion in a bovine serum albumin solution (A) 4.6 and (B) 9.2 µM) and (C) CV of $TiCp_2$-SBA-15 /graphite electrode before and 5 minutes after immersion in a bovine serum albumin solution 4.6 and 9.2 µM, In aqueous phosphate buffer pH 7.4 as electrolyte *vs* Ag/AgCl/KCl (3 M) as reference electrode.

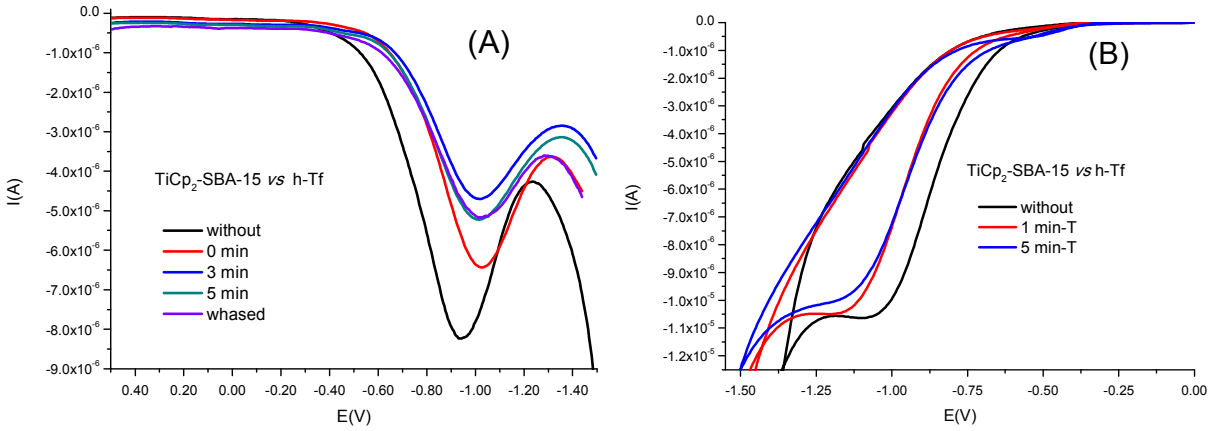

Figure 12. (A) DPV (75 mV modulation amplitude) and (B) CV of $TiCp_2$-SBA-15 /graphite electrode 5 min after immersion in transferrin solution in aqueous phosphate buffer pH 7.4 as electrolyte *vs* Ag/AgCl/KCl (3 M) as reference electrode.

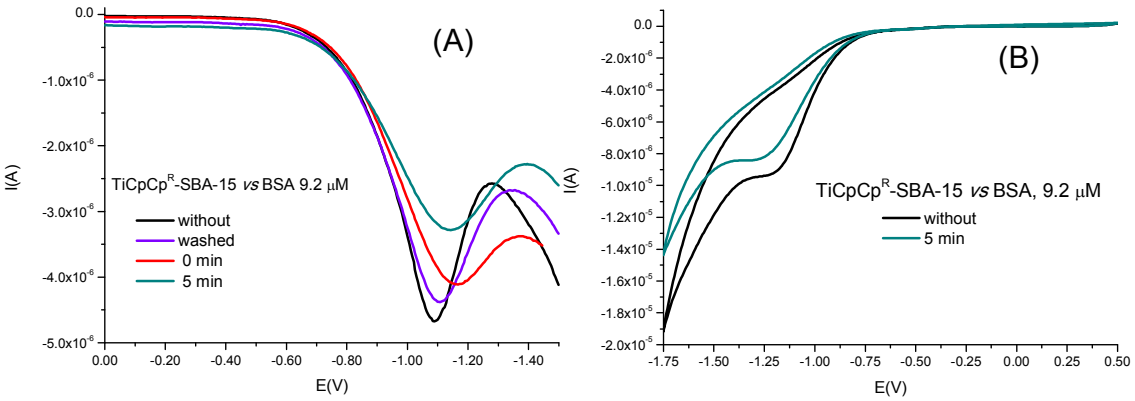

Figure 13. (A) DPV (75 mV modulation amplitude) and (B) CV (100mV/s) voltammograms of TiCpCp^R-SBA-15 /graphite electrode 5min after immersion in a bovine serum albumin solution 9.2 µM, in aqueous phosphate buffer pH 7.4 as electrolyte *vs* Ag/AgCl/KCl (3 M) as reference electrode.

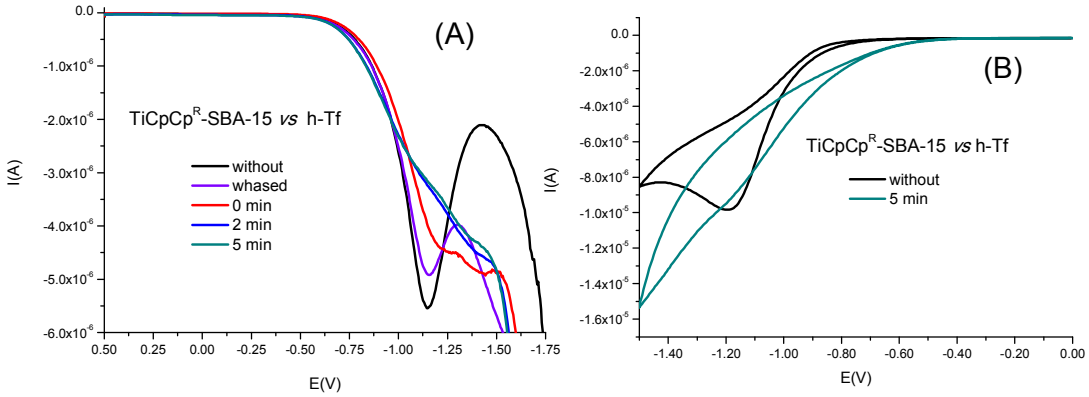

Figure 14. (A) DPV (75 mV modulation amplitude) and (B) CV of TiCpCp^R-SBA-15 /graphite electrode 5 min after immersion in transferrin solution in aqueous phosphate buffer pH 7.4 as electrolyte *vs* Ag/AgCl/KCl (3 M) as reference electrode.

An additional study was carried out using $TiCp_2$-SBA-15 and h-Tf. Figure 12 shows the DPV and CV voltammograms of $TiCp_2$-SBA-15 in the presence of an h-Tf solution in phosphate buffer used as electrolyte. In the DPV, the signal at -0.95 V previously attributed to the

tetracoordinated titanium complex grafted to the silica surface shifted to more negative potential, -1.06 V, and the current peak decreased gradually to reach a maximum and constant value of 5 minutes after transferrin contact. When the electrode surface was thoroughly washed with ultrapure water and a new measurement was recorded in pure buffer phosphate the signal remained constant. This profile can be interpreted as the initial interaction and following formation of a stable binding adduct between the "$TiCp_2$" moieties, resulting from tetra coordinated titanium complex at physiological pH and the hTf. Thus, "$TiCp_2$" moieties bound to hTf are protected from hydrolysis.[55] When conducting similar experiments with $TiCpCp^R$-SBA-15 in the presence of BSA and hTf (See Figures 13 and 14) the % interactions calculated on the basis of potential changes were not as strong as those observed for unsubstituted grafted titanocene (Table 4). This fact is also supported by the behaviour of $TiCpCp^R$-SBA-15 vs hTf after washing the electrode surface. New measurements showed that the initial signal is recovered.

These results show an interesting binding behaviour of the titanocene-functionalized materials with transport proteins such as albumin and transferrin with a higher affinity of the unsubstituted titanocene derivative $TiCp_2$-SBA-15 in comparison with $TiCpCp^R$-SBA-15. In addition, although the affinity towards transferrin or albumin seems to be very similar, the stability of the species obtained after interaction with transferrin (especially in the case of the supported unsubstituted titanocene derivative) is higher, pointing towards more robust systems based on hTf-Ti than on BSA-Ti.

2.3.3. Study of the interactions with guanosine and nucleic acids as models of cell targets of titanocene derivatives.

The use of electrochemical techniques in the study of metallodrugs-DNA interactions is very interesting due to the resemblance between electrochemical and biological reactions. The electrochemical methods are extremely sensitive and are mainly based on the differences in the redox behaviour of the binding molecules in the absence and presence of target molecules including the shifts of the formal potential of the redox couple and the decrease of the peak current resulting from the dramatic decrease in the diffusion coefficient after association with the molecule under scrutiny. Different studies have suggested that, in solution, titanocene binds to the active sites of DNA (such as oxygen sites of phosphates, nitrogen and oxygen sites of purine bases, etc,) to form chelate complexes. Previous reports have shown that for the cyclopentadienyl ligand its release is difficult mainly because the serum components seem to stabilize the "$TiCp_2$" moiety at physiological pH.[56]

In this section, differential pulse voltammetry measurements have also been used to study the binding ability of immobilized titanium complexes towards the nucleoside guanosine (GN), and nucleic acids single stranded DNA (s-DNA) and double stranded DNA (d-DNA) as models of target molecules for the titanium containing materials inside the cells. Figure 15A shows the differential pulse voltammograms recorded as a function of time of the modified carbon paste electrode with $TiCp_2$-SBA-15 in the presence of a solution of guanosine 4.0 mM in buffer phosphate at pH 7.4 as electrolyte. As can be seen, in the presence of guanosine 4.0 mM a new peak at -0.87 V appeared with lower peak current intensity, decreasing gradually with time to reach a constant peak current intensity after 5 minutes' adsorption time with the concentrated GN solution. After this time, the titanium-modified carbon paste electrode was removed from the guanosine solution and the surface thoroughly washed with ultrapure water, A new measurement by using pure buffer phosphate as electrolyte showed that the initial signal at -0.87 V is recovered. Additionally, as observed in Figure 15B, the amount of guanosine in solution has a linear relationship with the titanium reduction peak height. That is, there is a linear decrease in the titanium peak current peak on increasing the concentration of GN in solution within the concentration range of 0.04 to 1.0 mM. At concentrations higher than 1.0 mM, the response becomes non-linear which means that the interaction guanine-titanium at the electrode surface is limited by the saturation of the metallic active sites.

The dependence of interaction guanosine-material with the concentration is reflected in the % of titanium peak height change calculated by Equation 1. This value is 53 % and 62% for GN 1.0 and 4.0 mM, respectively. In the differential pulse voltammogram recorded for $TiCpCp^R$-SBA-15 at different concentration values of guanosine (Figure 16A), the cathodic peak associated to the reduction process of titanium slightly shifted to higher potential values. Again, the peak reduction height is concentration dependent, but the behaviour is nonlinear in a similar range of concentrations, probably due to the lower titanium loading of the studied material, as the surface may be saturated at small guanosine concentrations. The percentage interaction based on peak current variation at concentration 1.0 mM of GN was calculated to be 52%, lower that that obtained with $TiCp_2$-SBA-15 when reaching saturation of the reactive sites on the electrode surface. In addition, cyclic voltammetry studies support these results, as can be seen in Figure 16B which shows the CV recorded for $TiCpCp^R$-SBA-15 *vs* GN 4.0 mM, 5 minutes after immersion of the electrode into the aqueous solution. The peak current of the cathodic peak observed at 100 mV scan rate significantly decreased in the presence of the electron rich molecule.

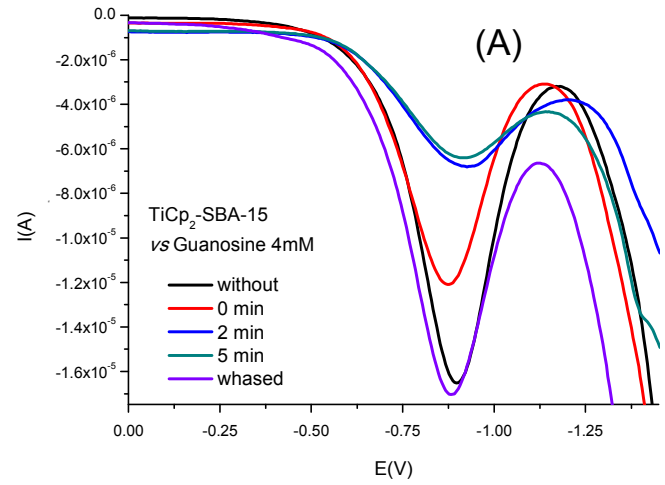

1

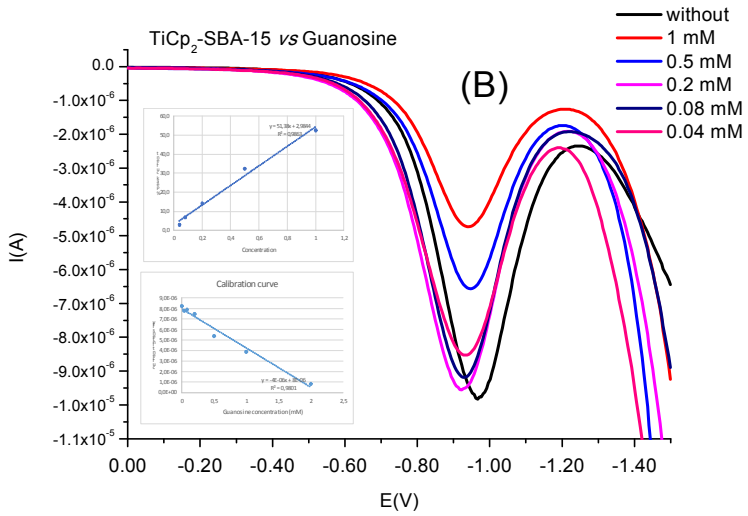

2

3 Figure 15. DPV (75 mV modulation amplitude) of $TiCp_2$-SBA-15 vs (A) Guanosine 4 mM at
4 different times after immersion (B) Guanosine concentrations in the range 1.0-0.04 mM in
5 aqueous phosphate buffer pH 7.4 as electrolyte vs Ag/AgCl/KCl (3 M) as reference electrode.
6 Linear plot of current peak height of titanium reduction vs concentration.

7

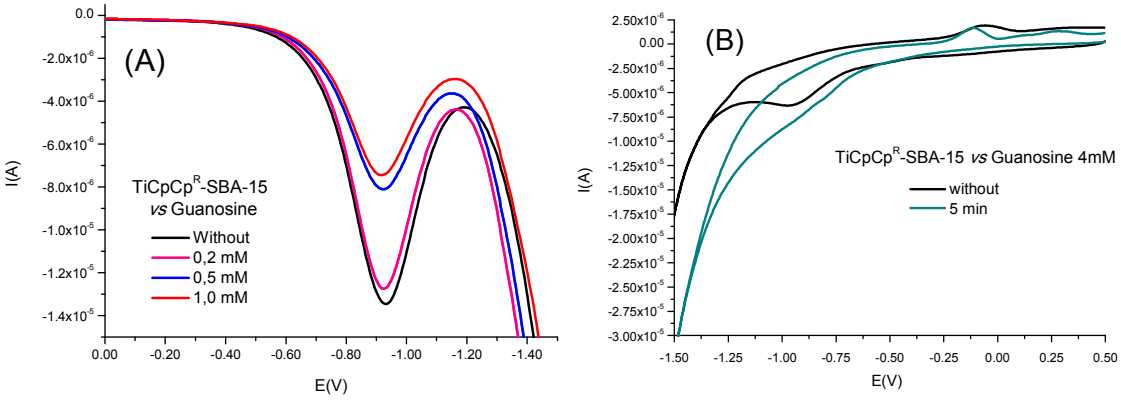

1

2 Figure 16. DPV (75 mV modulation amplitude) of TiCpCp^R-SBA-15 vs Guanosine concentrations
3 in the range 1.0-0.08 mM in aqueous phosphate buffer pH 7.4 (A) Guanosine 4mM at different
4 times after immersion (B) Cyclic voltammogram of TiCpCp^R-SBA-15 before a nd after 5 min
5 immersion into the aqueous guanosine 4mM solution using as electrolyte vs Ag/AgCl/KCl (3 M)
6 as reference electrode.

7 Previous studies have reported the ability of mesoporous silica-based materials to act
8 as biomolecules carriers, the physical adsorption of proteins was shown to be enhanced if the
9 pore diameter of the mesoporous support is similar in size to the macromolecule of biological
10 interest. Not only the pore diameter, but also the ordering of the pores, may interfere with
11 their adsorption capacity. In this context, Santos et al, have demonstrated that SBA-15 has the
12 pore size and specific pore volume needed to adsorb BSA and lysozyme (LYS), even though the
13 pore arrangement was poorly ordered.[57] In comparison with traditional SBA-15, the use of
14 SBA-15 with expanded pores and shorter channel lengths improves the biomolecule uptake of
15 BSA, LYS and cellulose.[58] Studies performed by Fantini and co-workers confirmed that BSA
16 protein has dimensions compatible with its incorporation within the mesopores of SBA-15 with
17 expanded pores. Nevertheless, with conventional SBA-15 with smaller pore size diameters (≈
18 38 Å), BSA covers the mouth of the pore and prevents the movement of the molecules into the
19 pore. [59,60]

20 In the studied materials, after titanocene immobilization the pore diameter decreases.
21 At this stage it is probable that most of the high dimension biomolecules used in this study are
22 attached to the external surface or at the pore mouth. Figures 17A and 17B show the DPV and
23 CV voltammograms of $TiCp_2$-SBA-15 recorded at different times in the presence of s-DNA and
24 d-DNA with two different concentrations, 0.018 and 0.092 mM. When studing the DPV, a

decrease in the peak current height associated to titanium was observed in all cases. This decrease is time dependent, but takes longer when compared with GN. Immediatily after immersion of the electrode into the DNA solution there was no change in the position or intensity of the cathodic peak. After 5 minutes adsorption time, the decrease in the peak current reached a maximum, For grafted titanocene derivatives, changes in the potential for the complex in the material and after the interaction have been used as indicators of the strength of interaction, since the potential is more sensitive to coordination environment than current. This interaction can be quantified using the following equation:

$$\%Interaction = \frac{E_{complex-drug} - E_{complex}}{E_{complex}} \times 100 \qquad \text{Eq. 2}$$

After 5 minutes contact $TiCp_2$-SBA-15 showed 2.8% interaction with s-DNA with both concentrated and diluted solutions. This interaction decreased to 1.6 % with concentrated and 0.4 % diluted d-DNA, gives evidence of a slightly more efficient interaction with more reactive single stranded DNA. Again, when the titanium modified carbon paste electrode was removed from the DNA solution and the surface thoroughly washed with ultrapure water, the new measurement by using pure buffer phosphate as electrolyte showed that the initial signal is recovered. In addition, a clear tendency was observed when taking into account the effect of DNA concentration; the current peak decrease is more important with more diluted concentrations. This behaviour is also supported by the cyclic voltammograms recorded after similar adsorption time periods at 100 mV/s scan rate. As previously discussed, the average pore size of the modified SBA-15 materials does not seem to be big enough to allow diffusion of the DNA into the mesopore, this effect is more influent at higher concentration values.

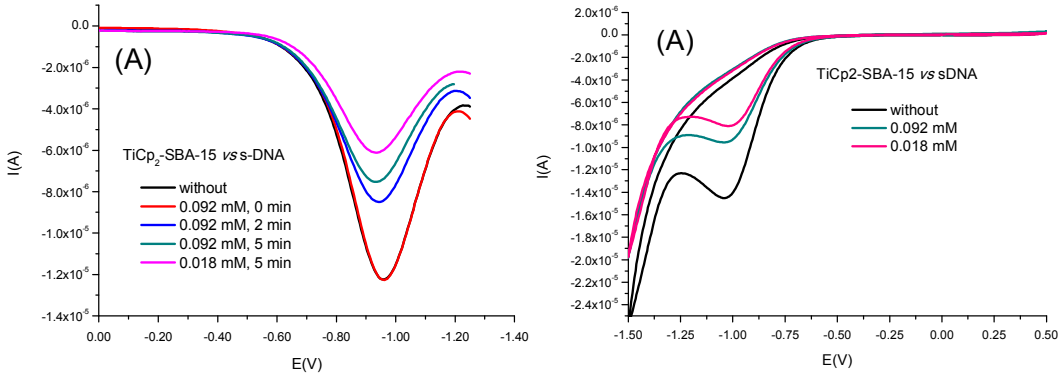

1

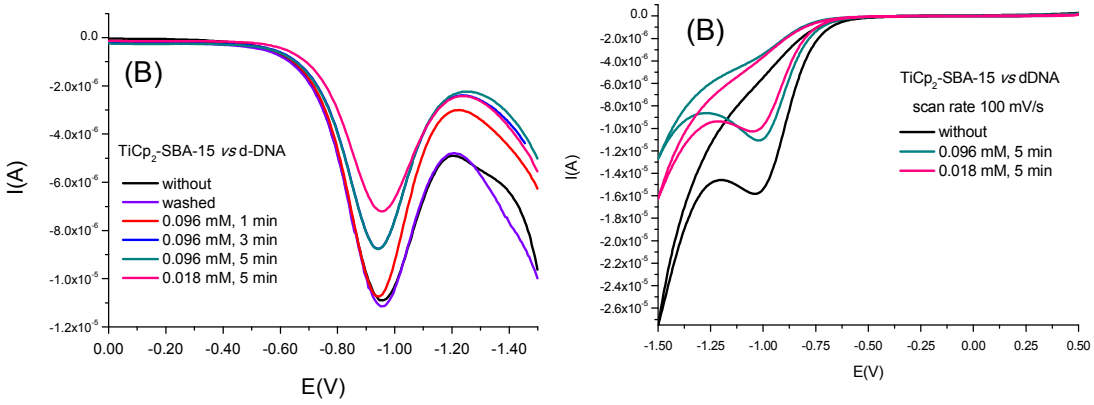

2

3 Figure 17. DPV (75 mV modulation amplitude) and cyclic voltammograms (100 mV/s scan rate)
4 of Ti-Cp_2-SBA-15 vs (A) single and (B) double strained DNA at different times after immersion
5 and concentrations 0.096 and 0.018 mM in aqueous phosphate buffer pH 7.4 as electrolyte vs
6 Ag/AgCl/KCl (3 M) as reference

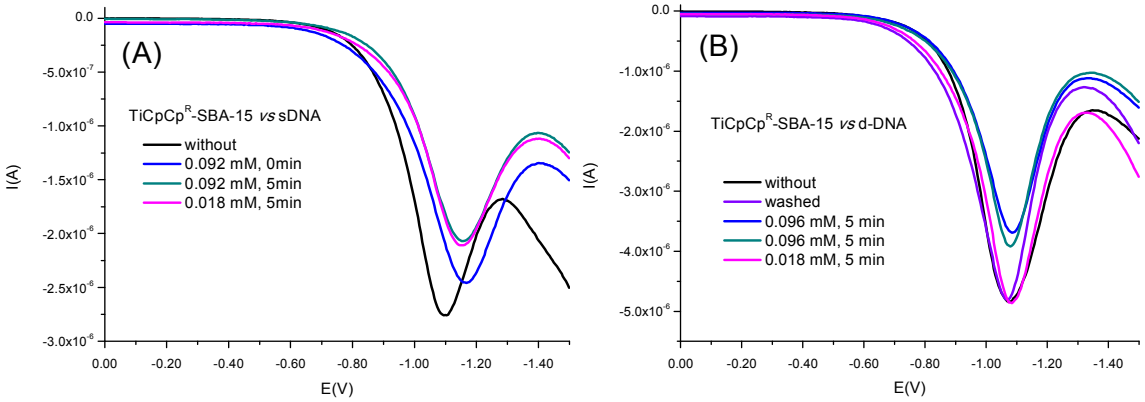

electrode.

Figure 18. DPV (75 mV modulation amplitude) of (A) TiCpCp^{R}-SBA-15 vs single and (B) double DNA at different times after immersion at concentrations of 0.092 and 0.018 mM in aqueous phosphate buffer pH 7.4 as electrolyte vs Ag/AgCl/KCl (3 M) as reference electrode.

When using TiCpCp^{R}-SBA-15 certain differences were observed (Figure 18). The cathodic peak diminished immediately after immersion in the DNA solution suggesting a rapid interaction. In the case of s-DNA, an important shift to more negative values of the potential was observed indicating an efficient coordination of titanium to more donating species. Again, the interaction is much more important at lower concentrations. On the contrary, with d-DNA solutions the decrease of the peak current increased with higher concentrations. The percentage of interaction based on potential changes was calculated to be 5.8 and 0.1 % for s-DNA and d-DNA, respectively. These results support less efficient interactions of this bulky substituted titanocene with double stranded DNA. When the titanium modified carbon paste electrode was removed from the DNA solution and the surface thoroughly washed with ultrapure water and a new measurement, using pure buffer phosphate as electrolyte, the initial signal was recovered. This behaviour was confirmed by the cyclic voltammograms recorded at 100 mV/s (See Figure S10).

For the targeting step, according to the electrochemical studies, materials functionalized with titanocene derivatives seem to strongly interact with a nucleoside like GN. However, the interaction with DNA (both s-DNA and d-DNA) is very low. Indeed, the titanocene-functionalized materials interact more weakly with d-DNA than with s-DNA. This is probably due to the difficulties in interacting with the nitrogenated bases of the double helix that are less accessible in the case of the double chain than that in the case of the single stranded system, In addition, as the degree of interaction appears to be very low in all cases and non-comparable with the strong interaction with GN, it seems clear that the size of the helixes and the relatively low accessibility of the nitrogenated bases of the DNA diminish their potential interaction indicating that DNA is unlikely to be attacked with facility by the supported titanium-containing metallodrugs. These results suggest that the DNA-attack by the materials is the limiting step in the cytotoxic action and point to biological targets other than DNA as real objectives of the titanocene-functionalized nanostructured systems. These electrochemical studies therefore support that the mechanism of cellular action and biological target of the titanocene-supported materials and the “free” titanocene complexes may be

different. It is generally agreed that the biological target in cells of the titanocene functionalized materials is probably DNA as reported by our group in recent studies.[12,15]

2.3.4. Ionic liquid influence in drug-biomolecule interactions

Since the results show that the ligands of the immobilized titanium complex affect its electronic properties and its ability to interact with molecules in solution; the next set of experiments focused on the search for information about the influence of the use of an IL bonded or interacting with the supported complex.[61] The choice of ILs was based on their versatile properties. The attachment of this ligand to the silica surface may diminish its hydrophobicity increasing silica materials and silica nanoparticles' ability to disperse in aqueous media. As previously deduced from the electrochemical studies in solution, ILs may also influence the redox properties of the titanium centre. Since the interaction of the metal-containing species grafted into the pores of the silica-based materials with molecules in solution is governed by the diffusion of these molecules into the pores, the presence of the ILs units needs to be analysed.

Solution-state studies have demonstrated that the effect of ILs is more pronounced in the redox properties of the classical unsubstituted titanocene complex. Thus, the material IMIL-TiCp$_2$SBA-15 has been chosen as a model to study the impact of the IMIL grafted onto the silica surface and its interaction with biomolecules. Firstly, a material with ILs immobilized into SBA-15 (IMIL-SBA-15) was studied and no peaks were observed with modified carbon paste electrode. Therefore, the peaks found for IMIL-TiCp$_2$SBA-15 have been assigned to the redox system Ti(IV)/Ti(III) demonstrating that titanium is readily accessible to electron transfer reactions in aqueous medium (See Figure S11). In the differential pulse voltammogram recorded for IMIL-TiCp$_2$-SBA-15 immediately after immersion of the graphite/silica working electrode into aqueous phosphate buffer pH 7.4 solution used as electrolyte, a peak associated to the reduction of grafted titanium(IV) complex was observed in the cathodic scan at -1.06 V. There was a clear shift of the peak to more negative potential values in comparison to that observed for TiCp$_2$-SBA-15 (without IL), which indicates higher electron density at the titanium atom when the IMIL is present. As can be seen in Figure 19, there is no difference between TiCp$_2$-IMIL-SBA-15 and IMIL-TiCp$_2$-SBA-15 reduction potential values suggesting that the synthetic procedure does not render different structural forms grafted onto the silica surface. To gain insight into the stability of the grafted titanium species against hydrolysis DP voltammograms have been recorded at different times. The profile obtained showed a decrease of the peak current observed at -1.06 V as a function of time. After 40 minutes a new signal at -1.01 V (shifted slightly from the original signal) was observed. This signal remained as

the only observable peak after two hours. This result suggests higher stability of titanocene species when IMIL is simultaneously tethered to the silica surface. The donor properties of the imidazolium unit and/or the presence of the chloride anion in the ionic liquid may influence the hydrolysis equilibrium; in solution it is well known that the equilibria associated with these species is heavily dependent upon pH and chloride concentration. The broadening of the peak can be explained by the loss of the mechanical properties of the graphite paste after the long period of immersion in the electrolyte solution. In addition, the effect of IMIL attached to the silica surface on the coordination environment of titanium was clearly demonstrated in solution by UV-Vis in the case of titanocene and by electrochemical techniques for both, substituted and unsubstituted titanocene. In the solid state the influence of IMIL leads to more negative reduction potential values for the couple Ti(IV)/Ti(III). As observed in previous studies of our group, the synthetic procedure affects clearly the amount of titanium loading onto the silica support. However, it can be concluded from the results obtained here, that the chemical nature of the grafted titanium species is unaffected.

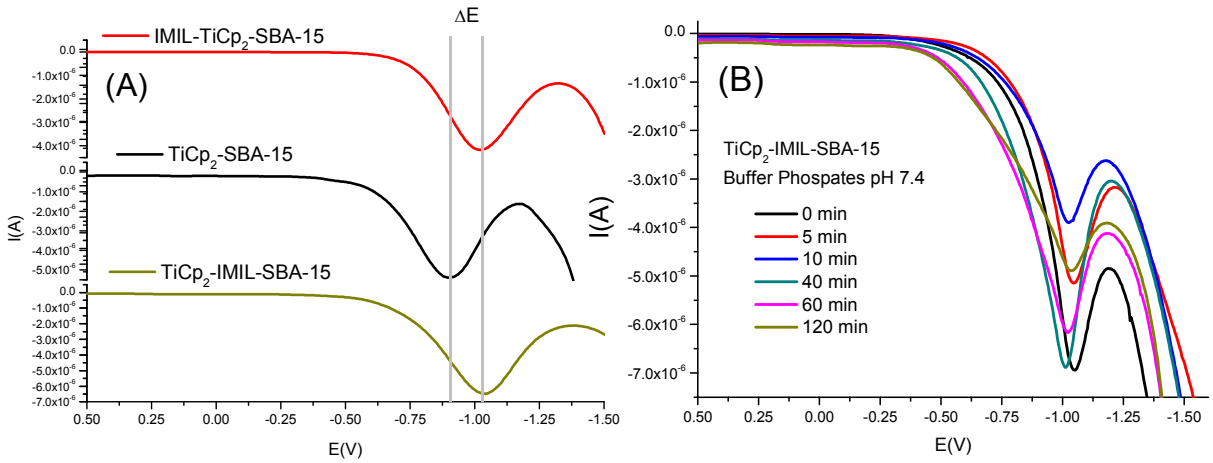

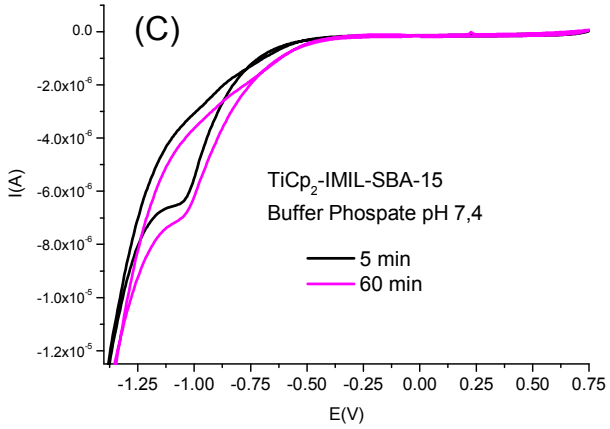

Figure 19. DPV (75 mV modulation amplitude) of (A) IMIL-$TiCp_2$-SBA-15 and $TiCp_2$-IMIL-SBA-15 in comparison to $TiCp_2$-SBA-15 (B) DPV and (C) CV of $TiCp_2$-IMIL-SBA-15 /graphite electrode as a function of time after immersion into the aqueous phosphate buffer pH 7.4 as electrolyte, *vs* Ag/AgCl/KCl (3 M) as reference electrode.

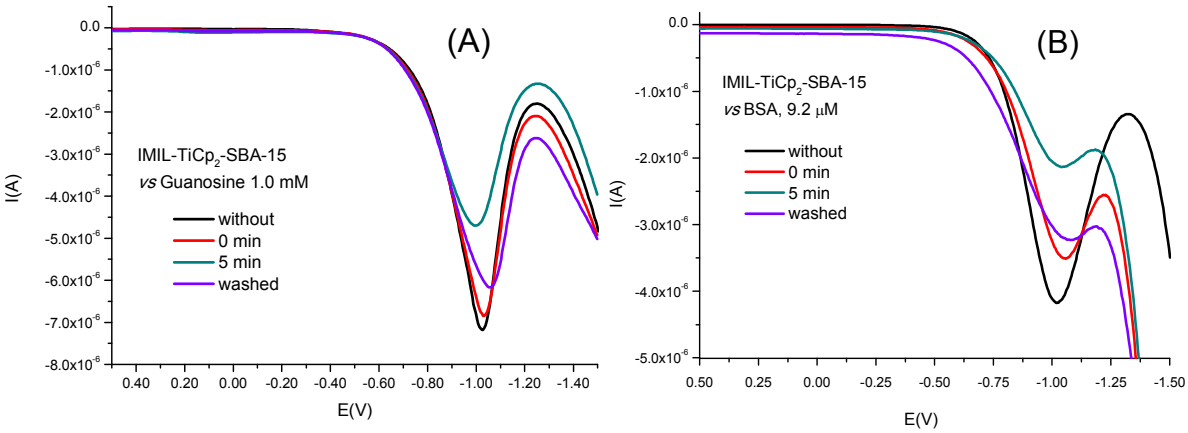

Figure 20. (A) DPV (75 mV modulation amplitude) of IMIL-$TiCp_2$-SBA-15 /graphite electrode after immersion into the aqueous Guanosine 1.0 mM as a function of time *vs* Ag/AgCl/KCl (3 M) as reference electrode, (B) DPV (75 mV modulation amplitude) of IMIL-$TiCp_2$-SBA-15/graphite electrode after immersion into BSA aqueous solution as a function of time *vs* Ag/AgCl/KCl (3 M) as reference electrode.

We have also studied the interaction of the IMIL-containing system IMIL-$TiCp_2$-SBA-15 with both BSA and guanosine as models of the transport proteins and biological targets inside

the cell, respectively. Figure 20 shows the differential pulse voltammograms recorded as a function of time of the modified carbon paste electrode with IMIL-$TiCp_2$-SBA-15 in the presence of a solution of guanosine 1.0 mM in buffer phosphate at pH 7.4 as electrolyte. As can be seen, immediately after immersion in the solution of guanosine the current peak decreased. When the electrode surface was thoroughly washed with ultrapure water and a new measurement recorded in pure buffer phosphate, the signal is not recovered. It is important to note that the opposite happens with $TiCp_2$-SBA-15. This can be interpreted to be due to the formation of a more stable binding adduct between the titanium complex at physiological pH and GN. After contact with a BSA solution and washing, the signal was recovered, but there was a significant decrease in comparison to the starting material, which can be interpreted again as the formation of a more stable binding adduct between the titanium complex at physiological pH and BSA. Finally, an additional study was carried out with IMIL-$TiCp_2$-SBA-15 and h-Tf where similar behaviour was observed (Figure 21). The main difference in comparison with guanosine or albumin is that, in the presence of transferrin, a slight shift to more negative potential values was observed. For comparison purposes the behaviour of $TiCp_2$-IMIL-SBA-15 vs transferrin has also been studied (Figure S12). There was no difference between $TiCp_2$-IMIL-SBA-15 and IMIL-$TiCp_2$-SBA-15 supporting the fact that, as previously observed, that the synthetic procedure incorporating IMIL before or after the grafting of the titanium complex does not render different structural forms grafted onto the silica surface.

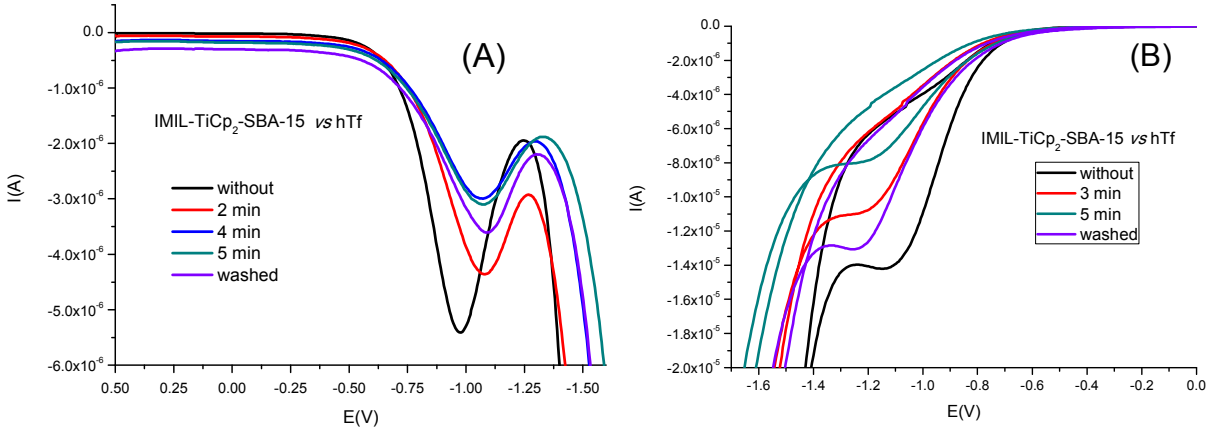

21

22

Figure 21. (A) DPV (75 mV modulation amplitude) and (B) CV of IMIL-$TiCp_2$-SBA-15/graphite electrode after immersion in transferrin solution in aqueous phosphate buffer pH 7.4 as electrolyte *vs* Ag/AgCl/KCl (3 M) as reference electrode.

Table 4. Change in potential (a) and current (b) for the electrochemical interaction of $TiCp_2$-SBA-15 and $TiCpCp^5$-SBA-15 vs biomolecules after surface electrode saturation (5 minutes time) in aqueous phosphate buffer pH 7.4.

Grafted complex	Biomolecule	Concentration	% interaction based on ΔE	% interaction based on ΔI
$TiCp_2$-SBA-15	**Guanosine**	1.0 mM	3.1	52.5
		4.0 mM	2.7	61.1
	s-DNA	0.018 mM	2.8	50.0
		0.092 mM	2.8	38.4
	d-DNA	0.019 mM	0.4	41.3
		0.096 mM	1.6	28.3
	BSA	4.2 μM	0.08	20.8
		9.2 μM	8.4	23.9
	h-Tf	50 mg/50mL	7.2	23.9
$TiCpCp^R$-SBA-15	**Guanosine**	1.0 mM	0.9	45.2
	s-DNA	0.018 mM	5.7	23.8
		0.092 mM	5.8	24.8
	d-DNA	0.019 mM	0.3	0.4
		0.096 mM	0.1	18.9
	BSA	9.2 μM	4.8	29.5
	h-Tf	50 mg/50mL	6.5	20.1
IMIL-$TiCp_2$-SBA-15	**Guanosine**	1.0 mM	2.8	34.4
	BSA	9.2 μM	2.5	48.7
	h-Tf	50 mg/50mL	11.7	43.9

2.4. Qualitative comparison of the interactions between biomolecules and titanocene supported materials

In the current study, a comparison of the experimental results from a quantitative point of view is not possible owing to the different scales units employed (concentration of biomolecules, titanium loading, etc,). However, the data can be analysed from a qualitative point of view and some clear conclusions about the affinity of materials for the biomolecules under study can be drawn.

As recently reviewed by Valentine and co-workers, studies of titanium complexes as anticancer drugs have always included metal-nucleic acid and metal-serum/transport protein interactions.[62] Titanocene interactions with DNA through binding with nucleotides have been

found to be very weak near pH 7.0. In this study, we have demonstrated that grafted titanocene derivatives present on the silica surface after the first hydrolysis step in $TiCp_2$-SBA-15 and $TiCpCp^R$-SBA-15, bind unambiguously at physiological pH values with small electron rich molecules such as guanosine. Taking into account the experimental approach used in this study, based on electrochemical biosensor techniques, this interaction is both time and concentration dependent. A linear relationship is observed between the calculated percentage of interaction based on peak current changes (before and after guanosine contact) and increasing concentrations values. The linear range observed has also been linked to the titanium loading on the silica surface, since a saturation effect on the silica surface is clearly observed. The interaction Ti-guanosine has demonstrated to be labile enough to allow the recovery of the initial titanium species after guanosine removal. The % percentage interaction calculated on the basis of reduction potential value offers more useful information about the coordination environment of titanium after guanosine interaction. The ΔE values are 3.5 and 0.9 % for $TiCp_2$-SBA-15 and $TiCpCp^R$-SBA-15, respectively (Table 4), showing a lower affinity of the substituted titanocene compound compared with the classical titanocene dichloride. In addition, the ΔE was lower for the grafted complex with the substituted cyclopentadienyl ring than for the unsubstituted titanocene complex. This fact indicates that the hydrolysis process did not induce, at this stage, the loss of the Cp rings attached to the grafted titanium complex and that they remain bonded to the metal centre during the interaction with guanosine.

The extended study, including the interaction at physiological pH of both materials with s-DNA and d-DNA, showed more affinity with the more reactive s-DNA, as demonstrated by the % interaction calculated on the basis of potential value changes. When comparing the metallic precursor immobilized, these ΔE values are 2.8 and 5.7 % for $TiCp_2$-SBA-15 and $TiCpCp^R$-SBA-15 with s-DNA (0.019 mM), respectively, indicating an important influence of the metallic species grafted onto the silica surface on the binding behaviour. However, in this study it was not possible to determine or differentiate the binding modes (stacking, hydrogen binding or ionic interactions) and effectiveness of interaction Ti-DNA. Nevertheless, the data suggest that the interaction is labile since the initial species were recovered after DNA removal. The effect of DNA concentration has also been studied and suggests an important role for the silica support. The nanostructured porous materials with smaller pore sizes after functionalization do not easily allow the free diffusion of DNA and the macromolecule seems to be located at the pore mouth of the nanostructured systems.

In the case of the interaction of titanocene-functionalized materials with BSA, as expected, the % interaction calculated on the basis of potential reduction changes was higher

than those previously obtained for GN and DNA. These values increased to 8.4 and 4.8% with BSA 9.2 μM for $TiCp_2$-SBA-15 and $TiCpCp^R$-SBA-15, respectively. However, the interaction was eliminated by BSA removal. On the other hand, in the presence of transferrin, the degree of interaction was 7.4 and 6.5 % for $TiCp_2$-SBA-15 and $TiCpCp^R$-SBA-15; respectively. It seems clear in both cases that a more efficient interaction is established between proteins and unsubstituted titanocene species. Important data were obtained when examining the behaviour of these materials after protein removal, namely, the signal due to initial titanium species was clearly recovered in the study of both materials after the appropriate work up with BSA. However, in the presence of transferrin the new signal observed for $TiCp_2$-SBA-15, shifted to more negative values and with the lower value of peak current, remains unaltered, which supports the formation of a stable coordination adduct. This behaviour does not hold true for $TiCpCp^R$-SBA-15; as with this complex the signal attributed to tetrahedral Ti(IV) species was clearly recovered after transferrin removal from the experimental media. These results may indicate a higher stability that in spite of the lower affinity of $TiCpCp^R$-SBA-15 the transportation steps may be more effective because the release of the titanium containing species from the transferrin inside the cell may be easier than in the case of $TiCp_2$-SBA-15.

In addition, as previously observed, the presence of IMIL attached to the silica surface affects the coordination environment of the titanium centre increasing its electron density and making more negative the reduction potential values of the couple Ti(IV)/Ti(III). The degree of interaction calculated based on the ΔE showed comparable values (slightly lower and shifted to more positive values) to those obtained with $TiCp_2$-SBA-15. These values are 2.8 and 2.5 % for GN 1.0 mM and BSA (9.2 μM), respectively with IMIL-$TiCp_2$-SBA-15, *vs* 3.1 and 2.8 % interaction for the mentioned $TiCp_2$-SBA-15. On the contrary, the % interaction calculated based on the differences of peak current intensity significantly changed. It seems than the presence of the ionic liquid does not exert a clear influence on the nature of the titanium-biomolecule interaction, but it affects the extent of it. The % interaction for guanosine 1.0 mM decreased from 52.5 % with $TiCp_2$-SBA-15 to 34.4 % with IMIL-$TiCp_2$-SBA-15, but it nearly doubled with both proteins BSA (9.2 μM) and hTf. With the latter protein the trend was also the same to that previously observed with other materials, giving the highest values of % interaction based on ΔE in comparison with the rest of the studied biomolecules. Since the amount of titanium loading on both materials, $TiCp_2$-SBA-15 and IMIL-$TiCp_2$-SBA-15 is similar, the differences in % interaction based on ΔI must be due to the presence of the ionic liquid on the silica surface.

Furthermore, when the electrode surface of the graphite paste electrode prepared with IMIL-$TiCp_2$-SBA-15 was thoroughly washed and new measurements were recorded by using fresh electrolyte, the signal attributed to titanium species grafted onto the silica material were recovered when using guanosine as target molecule. Contrarily, in the presence of both BSA and hTf, the peak intensity slightly increased but there were no changes in the potential value. The titanium-biomolecule adduct seems to be stable, but the extent of the interaction decreases, It can be affirmed that IMIL increases the stability of the titanium-biomolecule adducts in comparison with the material which does not contain IMIL. In a recent study Masuda and co-workers have observed that non-coordinating ionic liquids promote N_2 coordination to Ti(III).[63]

3. Conclusions

In this study we have observed that, in the presence of molecules of biological interest, titanium immobilized mesoporous silica materials exhibit a reduction peak attributed to the couple Ti(IV)/Ti(III) with an obvious decrease in the diffusion currents and the reduction of the titanium-drug species shifts to more negative potential. The enhanced diffusion current in the absence of drugs indicates the titanium-biomolecule association. In addition, the slight cathodic shift in the corresponding E_{red} value which can be attributed to the reduction of the more stabilized adduct upon interaction with the biomolecule.

The electrochemical study has shown the higher stability of $TiCpCp^R$-SBA-15 compared with that of $TiCp_2$-SBA-15 in physiological medium, and a higher degree of interaction of $TiCp_2$-SBA-15 with BSA, h-Tf and DNA compared with $TiCpCp^R$-SBA-15 indicating that the speciation process of the titanocene-functionalized materials plays an important role in determining their cytotoxic activity.

In addition, the transport processes associated with the action of the titanocene-functionalized SBA-15 materials may be mediated by both h-Tf or albumin as the differences in affinity are not very significant. However, the limiting step for the cytotoxic action of these materials may be the attack on DNA as the electrochemical study has demonstrated a low degree of interaction with both s-DNA and d-DNA. Thus, the results show that the mechanism of cellular action and biological target of the titanocene-supported materials and the “free” titanocene complexes are different and the materials promote cancer cell death by action against other metabolites of the cells and not DNA as suggested in previous cytotoxic studies of our group performed for similar materials.[12,15]

Finally, our study has demonstrated the important influence of the incorporation of an ionic liquid such as IMIL on the titanocene-functionalized silica-based materials which is crucial for improving the binding and stability of the materials for biological applications.

4. Conflict of Interest

The authors have no conflicts to declare.

5. Acknowledgements

We gratefully acknowledge financial support from the MICINN (project CTQ2015-66164-R) and Universidad Rey Juan Carlos-Banco Santander (Excellence group QUINANOAP).

References

1. H. Köpf, P. Köpf-Maier, Angew. Chem. Int. Ed. **1979**, 18, 477–478.
2.S. Gómez-Ruiz, D. Maksimović-Ivanic, S. Mijatović, G. N. Kaluderović, *Bioorg. Chem. App.* **2012**, 140284.
3. Y. Ellahioui, S. Prashar, S. Gómez-Ruiz, *Inorganics* **2017**, *5*, 4.
4. G. Palma, M. D'Aiuto, D. Rea, S. Bimonte, R. Lappano, M.S. Sinicropi, M. Maggiolini, P. Longo, C. Arra, C. Saturnino, *Biochem-Pharma.* **2014**, *3*, 1–12.
5. T. Kiss, E. A. Enyedy, T. Jakusch, *Coord. Chem. Rev.* **2017**, *352*, 401–423.
6. W. Wani, S. Prashar, S. Shreaz, S. Gómez-Ruiz, *Coord. Chem. Rev.* **2016**, *312*, 67–98.
7. Y. Ellahioui, S. Prashar, S. Gómez-Ruiz, *Curr. Med. Chem.* **2016**, *23*, 4450–4467.
8. D. Pérez-Quintanilla, S. Gómez-Ruiz, Z. Žižak, I. Sierra, S. Prashar, I. del Hierro, M. Fajardo, Z. D. Juranić, G. N. Kaluđerović, *Chem. Eur. J.* **2009**, *15*, 5588–5597.
9. G. N. Kaluđerović, D. Pérez-Quintanilla, I. Sierra, S. Prashar, I. del Hierro, Z. Žižak, Z. D. Juranić, M. Fajardo, S. Gómez-Ruiz, *J. Mater. Chem.* **2010**, *20*, 806–814.
10. G. N. Kaluđerović, D. Pérez-Quintanilla, Z. Žižak, Z. D. Juranić, S. Gómez-Ruiz, *Dalton. Trans.* **2010**, *39*, 2597–2608.
11. A. García-Peñas, S. Gómez-Ruiz, D. Pérez-Quintanilla, R. Paschke, I. Sierra, S. Prashar, I. del Hierro, G. N. Kaluđerović, *J. Inorg. Biochem.* **2012**, *116*, 100–110.
12. J. Ceballos-Torres, P. Virag, M. Cenariu, S. Prashar, M. Fajardo, E. Fischer-Fodor, S. Gómez-Ruiz, *Chem. Eur. J.* **2014**, *20*, 10811–10828.
13. J. Ceballos-Torres, S. Prashar, M. Fajardo, A. Chicca, J. Gertsch, A. B. Pinar, S. Gómez-Ruiz, *Organometallics* **2015**, *34*, 2522–2532.
14. M. Z. Bulatović, D. Maksimović-Ivanić, C. Bensing, S. Gómez-Ruiz, D. Steinborn, H. Schmidt, M. Mojić, A. Korać, I. Golić, D. Pérez-Quintanilla, M. Momčilović, S. Mijatović, G. N. Kaluđerović, *Angew. Chem. Int. Ed.* **2014**, *53*, 5982–5987.
15. S. Gómez-Ruiz, A. García-Peñas, S. Prashar, A. Rodríguez-Diéguez, E. Fischer-Fodor, *Materials*, **2018**, *11*, 224.
16. J. Ceballos Torres, I. del Hierro, S. Prashar, M. Fajardo, S. Mijatović, D- Maksimović-Ivanić, G. N. Kaluđerović, S. Gómez Ruiz, *J. Organomet. Chem.* **2014**, *769*, 46–57.

17. M. Ravera, G. Bagni, M. Mascini, D. Osella, *Bioinorg. Chem. Appl.* **2007**, 91078.
18. I. del Hierro, Y. Pérez, P. Cruz, R. Juárez, *Eur. J. Inorg. Chem.* **2017**, *24*, 3030–3039.
19. S. Siddiquee, K. Rovina, N.A Yusof, K.F. Rodrigues, S. Suryani, Sens. Biosens. Research. **2014**, *2*, 16–22.
20. X. Zhou, T. Wu, K. Ding, B. Hu, M. Hou, B. Han, *Chem. Commun.* **2009**, 1897–1899.
21. M. Mazloum-Ardakani, A. Hoshroo, *Anal. Chim. Acta,* **2013**, *798*, 25–32.
22. E. Monti, M. B. Gariboldi, R. Ravizza, R. Molteni, K. Sparnacci, M. Laus, E. Gabano, M. Ravera, D. Osella, *Inorg. Chim. Acta* **2009**, *362*, 4099–4109.
23. N. L. Dias Filho, *Colloids Surf. A: Physicochem. Eng. Aspects,* **1998**, *144*, 219–227.
24. S. Bai, X. Hu, J. Sun, B. Ren, *New. J. Chem.* **2014**, *38*, 2128–2134.
25. Y. Mugnier, C. Moise, E. Laviron, *J. Organomet. Chem.* **1981**, *210*, 69–72.
26. R. J. Enemærke, J. Larsen, T. Skrydstrup, K. Daasbjerg, *Organometallics* **2004**, *23*, 1866–1874.
27. T. Fuchigami, *ECS Trans.* **2010**, *25*, 1–11.
28. M. A. Vorotyntsev, M. Casalta, E. Pousson, L. Roullier, G. Boni, C. Moise, *Electrochem. Acta* **2001**, *46*, 4017-4033.
29. M. Guo, H. Sun, H. J. McArdle, L. Gambling, P. J. Sadler, *Biochemistry* **2000**, *39*, 10023–10033.
30. A. D. Tinoco, E. V. Eames, A. M. Valentine, *J. Am. Chem. Soc.* **2008**, *130*, 2262–2270.
31. E. Paleček, M. Bartošík, *Chem. Rev.* **2012**, *112*, 3427–3481.
32. S. Rauf, J. J. Gooding, K. Akhtar, M. A. Ghauri, M. Rahman, M. A. Anwar, A. M. Khalid, *J. Pharmaceutical. Biomed. Anal.* **2005**, *37*, 205-217.
33. F. Arjmand, M. Aziz, S. Tabassum, *Curr. Anal. Chem.* **2011**, *7*, 71-79.
34. M. Ravera, E. Gabano, S. Baracco, D. Osella, *Inorg. Chim. Acta.* **2009**, *362*, 1303–1306.
35. C. J. P. Siburt, E. M. Lin, S. J. Brandt, A. D. Tinoco, A. M. Valentine, A. L. Crumbliss, *J. Inorg. Biochem.* **2010**, *104*, 1006–1009.
36. M. Shen, J. Wang, M. Tang, G. Li, *Electrochem. Commun.* **2011**, *13*, 114–116.
37. M. Ravera, E. Gabano, M. Sardi, M. Alessio, D. Osella, *Eur. J. Inorg. Chem.* **2011**, 1635–1639.
38. A. J. Santiago-López, J. L. Vera, E. Meléndez, *J. Electroanal. Chem.* **2014**, *731*, 139–144.
39. L. de Miguel, G. Cebrián-Torrejón, E. Caudron, L. Arpinati, A. Doménech-Carbó, G. Ponchel. Chem. *Electro. Chem.* **2015**, *2*, 748–754.
40. V. Brabec*, Electrochim. Acta* **2000**, *45*, 2929–2932.
41. I. del Hierro, Y. Pérez, M. Fajardo, *J. Solid State Electrochem.* **2015**, *19*, 2063–2074.
42. J.H. Toney, T.J. Marks, *J. Am. Chem. Soc.* **1985**, *107*, 947–953.
43. M. M. Harding, G. Mokdsi, *J. Organometal. Chem.* **1998**, *565*, 29–35.
44. M. M. Harding, J. H. Murray, *J. Med. Chem.* **1994**, *37*, 1936–1941.
45. M. Lovric, F. Scholz, *J. Solid State Electrochem.* **1997**, *1*, 108–113.
46. M. Lovric, F. Scholz, *J. Solid State Electrochem.* **1999**, *3*, 172–175.
47. K. B. Oldham, *J. Solid State Electrochem.* **1998**, *2*, 367–377.
48. I. M. M. Fussing, D. Pletcher, R. J. Whitby, *J. Organomet. Chem.* **1994**, *470*, 109–117.
49. M. Napoli, C. Saturnino, E. Sirignano, A. Popolo, A. Pinto, P. Longo, *Eur. J. Med. Chem.* **2011**, *46*, 122–128.
50. P. M. Abeysinghe, M. M. Harding, *Dalton Trans.* **2007**, 3474–3482.
51. D. Osella, M. Ravera, C. Floriani, E. Solari, *J. Organomet. Chem.* **1996**, *510*, 45–50.

52. A. R. Timerbaev, C. G. Hartinger, S. S. Aleksenko, B. K. Keppler, *Chem. Rev.* **2006**, *106*, 2224–2248.
53. T. Topală, A. Bodoki, L. Oprean, R. Oprean, *Clujul Med.* **2014**, *87*, 215–219.
54. I. Feliciano, J. Matta, E. Meléndez, *J. Biol. Inorg. Chem*. **2005**, 14, 1109-1117.
55. M. Pavlaki, K. Debeli, I.E. Triantaphyllidou, N. Klouras, E. Giannopoulou, A.J. Aletras, *J. Biol. Inorg. Chem.* **2009**, *14*, 947–957.
56 C. Deng, L. Zhou, *Inorg. Chim. Acta* **2011**, *370*, 70–75.
57 S. M. L. Santos, K. A. B. Nogueira, M. S. Gama, J. D. F. Lima, I. J. Silva Jr., D. C. S. Azevedo, *Micropor. Mesopor. Mater.* **2013**, *180*, 284–292.
58. S. M. L. Santos, J. A. Cecilia, E. Vilarrasa-García, I. J. Silva Jr., E. Rodríguez-Castellón, D. C. S. Azevedo, *Micropor. Mesopor. Mater.* **2016**, *232*, 53–64.
59. P. R. A. F. García, R. N. Bicev, C. L. P. Oliveira, O. A. Sant'Anna, M. C. A. Fantini, *Micropor. Mesopor. Mater.* **2016**, *235*, 59–68.
60. T. P. B. Nguyen, J.-W. Lee, W. G. Shim, H. Moon, *Micropor. Mesopor. Mater.* **2008**, *110*, 560–569.
61. R. Ballesteros, M. Fajardo, I. Sierra, C. Force, I. del Hierro, *Langmuir* **2009**, 25, 12706–12712.
62. K. M. Buettner, A. M. Valentine, *Chem. Rev.* **2012**, *112*, 1863–1881.
63. A. Katayama, T. Inomata, T. Ozawa, H. Masuda, *Dalton Trans.* **2017**, *46*, 7668–7671.

Supporting Information

Mesoporous SBA-15 Modified with Titanocene Complexes and Ionic liquids: Interactions with DNA and other Molecules of Biological Interest Studied by Solid State Electrochemical Techniques.

Isabel del Hierro*, Santiago Gómez-Ruiz*, Yolanda Pérez, Paula Cruz, Sanjiv Prashar, Mariano Fajardo.

Departamento de Biología y Geología, Física y Química Inorgánica, ESCET, Universidad Rey Juan Carlos. Calle Tulipán S/N, E-28933 Móstoles (Madrid) Spain.

1. Experimental Section

1.1. Reagents and solutions

The chemicals used in this study tetraethylortosilicate (TEOS) 98%, Poly(ethylene glycol)-block-poly(propylene glycol)-block-poly(ethylene glycol) (Pluronic P123, M_{av} = 5800), tetraethoxysilane, 98% (TEOS), (3-chloropropyl)triethoxysilane, 95% (CPTS), titanocene [Ti(η^5-$C_5H_5)_2Cl_2$], guanosine (G), bovine serum albumin (BSA), single-stranded DNA of fish sperm (s-DNA) and double stranded DNA of fish sperm (d-DNA) and transferrin were purchased from (Sigma-Aldrich) and used as received, without further purification. Organic solvents were purchased from VWR. They were distilled and dried before use, when needed, according to conventional literature methods. [1] Buffer phosphate solutions were prepared using KH_2PO_4 and Na_2HPO_4, HCl 35% (Scharlau) and ultrapure water (Milli-Q, Micropore). The hexagonal material (SBA-15) was prepared using a poly (alkaline oxide) triblock copolymer surfactant in acidic medium, according to the method of *Zhao et al.* [2] The ionic liquid 1-methyl-3-[(triethoxysilyl)propyl]imidazolium chloride (IMIL)[3] and the lithium compound Li{C_5H_4(CMePh($CH_2CH_2CH=CH_2$))} [**Error! Bookmark not defined.**] were synthesized following reported procedures.

1.2. Characterization

X-ray diffraction (XRD) patterns of the silica were obtained on a Philips Diffractometer model PW3040/00 X'Pert MPD/MRD at 45 KV and 40 mA, using Cu-Kα radiation (λ = 1.5418 Å). N_2 gas adsorption-desorption isotherms were obtained using a Micromeritics ASAP 2020 analyser, and pore size distributions were calculated using the Barret-Joyner-Halenda (BJH) model on the adsorption branch. Infrared spectra were recorded on a Nicolet-550 FT-IR spectrophotometer (in the region 4000 to 400 cm^{-1}) as nujol mulls between polyethylene

pellets and KBr disks. ^{13}C-CP MAS NMR (4.40 μs 900 pulse, spinning speed of 6 MHz, pulse delay 2 s) spectra were recorded on a Varian-Infinity Plus Spectrometer at 400 MHz operating at 100.52 MHz proton frequency. X-Ray Fluorescence Spectroscopy (XRF, Philips Analytical) was employed to determine the quantity of titanium in the functionalized materials. The DRUV-Vis spectroscopic measurements were carried out on a Varian Cary-500 spectrophotometer equipped with an integrating sphere and polytetrafluoroethylene (PTFE) as reference, with d = 1 g cm^{-3} and thickness of 6 mm. The cyclic voltammograms were recorded with a potentiostat/galvanostat Autolab PGSTAT302 Metrohm. A conventional three electrode system was used throughout the electrochemical experiments at the room temperature with a modified carbon paste electrode (CPE) as working electrode, a platinum wire as auxiliary electrode, and a saturated Ag/AgCl/KCl (3 M) electrode (Metrohm) as reference electrode against which all potentials were measured. The phosphate buffer used as electrolyte solution in the cell was purged with high purity nitrogen gas for at least 5 min to remove dissolved oxygen and then a nitrogen atmosphere was kept over the solution during measurements.

1.3. Synthesis of materials

1.3.1. Synthesis of [Ti(η^5-C_5H_5){η^5-C_5H_4(CMePh($CH_2CH_2CH=CH_2$))}Cl_2].

A solution of Li{C_5H_4(CMePh($CH_2CH_2CH=CH_2$))} (1.00 g, 4.35 mmol) in THF (50 mL) was added dropwise during 15 min to a solution of [Ti(η^5-C_5H_5)Cl_3] (0.91 g, 4.15 mmol) in THF (50 mL) at 0 ^{o}C. The reaction mixture was allowed to warm to room temperature and stirred for 2 h, Solvent was removed *in vacuo* and a toluene / hexane 9:1 mixture (50 mL) added to the resulting solid. The suspension was filtered and the filtrate concentrated (20 mL) and cooled to 30 ^{o}C to give the title compound as a red solid. Yield: 1.70 g, 81%, FT-IR (KBr): ν = 3096 cm^{-1} for νCH, 1638 (m) cm^{-1} for ν(C=C), ^{1}H NMR (400 MHz, $CDCl_3$, 25 ^{o}C): δ = 1.81 (s, 3H, CMePh), 2.08 (m, 2H, $CH_2CH_2CH=CH_2$), 2.36 (m, 2H, $CH_2CH_2CH=CH_2$), 4.92 (m, 2H, $CH_2CH_2CH=CH_2$), 5.75 (m, 1H, $CH_2CH_2CH=CH_2$), 6.08 and 6.44 (m, each 2H, C_5H_4), 6.15 (s, 5H, C_5H_5), 6.86 (t, 1H, H in para position of Ph), 7.26 (m, 2H, H in meta position of Ph), 7.37 (d, 2H, H in ortho position of Ph) ppm, ^{13}C{^{1}H} NMR (100 MHz, $CDCl_3$, 25 ^{o}C): δ = 23.7 and 28.7 ($CH_2CH_2CH=CH_2$), 42.2 (CMePh), 44.1 (CpC), 113.8 ($CH_2CH_2CH=CH_2$), 114.5, 117.2 and 144.9 (C_5H_4), 120.5 (C_5H_5), 121.9, 126.7, 127.4 and 128.4 (C_6H_5), 138.3 ($CH_2CH_2CH=CH_2$) ppm.

1.3.2. Preparation of SBA-15 functionalized with ionic liquid (IMIL-SBA-15).

The ionic liquid 1-methyl-3-[(triethoxysilyl)propyl]imidazolium chloride (IMIL) (1.3 g, 4 mmol) was dissolved in chloroform and added to 1.0 g SBA-15 (dehydrated at 150 ^{o}C in vacuum for 12 h). The mixture was refluxed at 80 ^{o}C for 24 h. The material was isolated by

filtration and washed with dichloromethane (3 x 30 mL) and hexane (1 x 30 mL). The resulting material, designated as IMIL-SBA-15, was dried under vacuum and store under inert atmosphere.

1.3.3. Immobilization of titanocene dichloride derivatives onto SBA-15, $TiCp_2$-SBA-15 and $TiCpCp^R$-SBA-15.

The titanium containing mesoporous material was prepared by reaction of $[Ti(\eta^5\text{-}C_5H_5)_2Cl_2]$ ($TiCp_2Cl_2$) or $[Ti(\eta^5\text{-}C_5H_5)\{\eta^5\text{-}C_5H_4(CMePh(CH_2CH_2CH{=}CH_2))\}Cl_2]$ ($TiCpCp^RCl_2$) with SBA-15. In a typical experiment, 1.5 g of SBA-15, previously dehydrated in vacuum at 110 ^oC for 12 h, was suspended in 30 mL of THF and a solution of $[Ti(\eta^5\text{-}C_5H_5)\{\eta^5\text{-}C_5H_4(CMePh(CH_2CH_2CH{=}CH_2))\}Cl_2]$ (0.100 g, 0.25 mmol) in 10 mL of THF was added. The suspension was stirred for 24 h at reflux temperature. The resulting pale orange solid, labelled as $TiCpCp^R$-SBA-15, was isolated by filtration and washed with dichloromethane (4 x 30 mL) until the washings became colourless in order to ensure the complete elimination of the non-immobilized titanocene derivative. The solid was dried under vacuum and stored under inert atmosphere.

1.3.4. Immobilization of titanocene dichloride derivatives onto IMIL-funcionalized SBA-15, $TiCp_2$-IMIL-SBA-15 and $TiCpCp^R$-IMIL-SBA-15.

The nanostructured materials containing titanocene complexes and ionic liquid were prepared by reaction of $TiCp_2Cl_2$ or $TiCpCp^RCl_2$ with SBA-15 previously functionalized with 1-methyl-3-[(triethoxysilyl)propyl]imidazolium chloride (IMIL). In a typical experiment, 1.0 g of IMIL-SBA-15, was suspended in 30 mL of THF and a solution of $TiCpCp^RCl_2$ (0.10 g, 0.25 mmol) in 10 mL of THF was added, The suspension was stirred for 24 h at reflux temperature. The resulting pale orange solid, labelled as $TiCpCp^R$-IMIL-SBA-15, was isolated by filtration and washed with dichloromethane (4 x 30 mL) until the filtrate until the washings became colourless in order to ensure the complete elimination of the excess of the titanocene derivative. The solid was dried under vacuum and stored under inert atmosphere.

1.4. Electrode preparation.

The modified carbon paste electrodes (MCPE) used as working electrode were prepared by mixing with a pestle in an agate mortar the previously modified mesoporous microspheres with graphite (Metrohm) (6-10% (w,w) ratio) and mineral oil as agglutinant (Sigma-Aldrich) until a uniform paste was obtained. The resulting material was packed into the end of a Teflon cylindrical tube equipped with a screwing stainless steel piston providing an inner electrical contact. All of the initial electrode activity could always be restored by simply

removing the outer layer of paste by treatment with polishing paper. DPV parameters were as follows: the initial potential of -1.0 V, the end potential -1.75 or -2.0 V, the modulation time 0.057 s, the time interval 0.2 s, the step potential 1.05 mV/s, the modulation amplitude of 75 mV.

2. Supplementary Figures

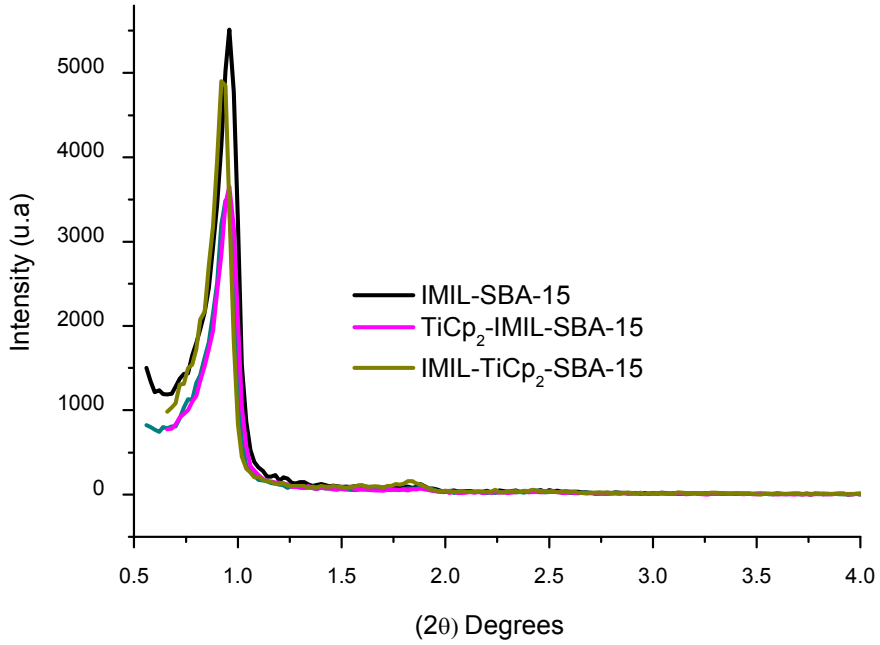

Figure S1. DRX patterns of IMIL-SBA-15, IMIL-$TiCp_2$-SBA-15 and $TiCp_2$-IMIL-SBA-15.

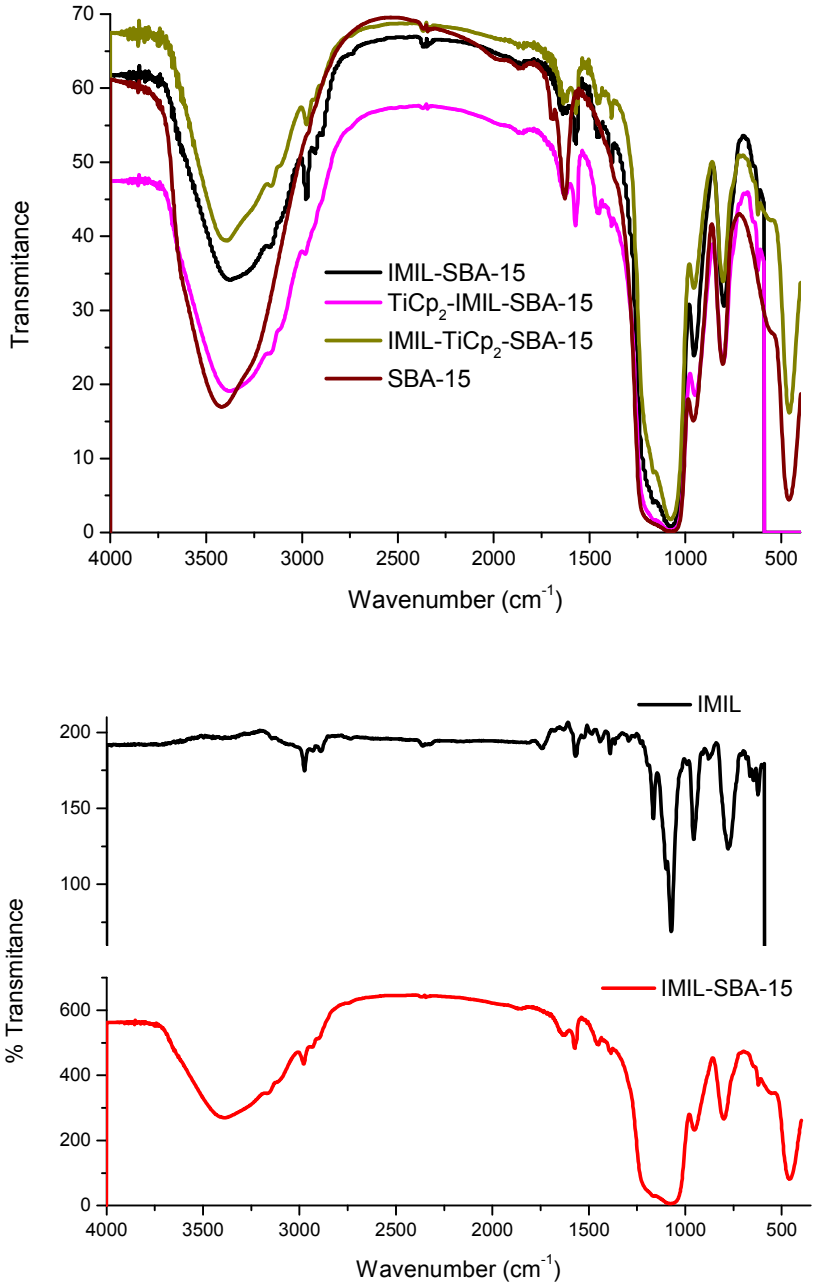

Figure S2. FTIR Spectra of SBA-15, IMIL-SBA-15, $TiCp_2$-SBA-15 and IMIL-$TiCp_2$-SBA-15, and FTIR of 1-methyl-3-[(triethoxysilyl)propyl]imidazolium chloride (IMIL) in comparison to IMIL-SBA-15.

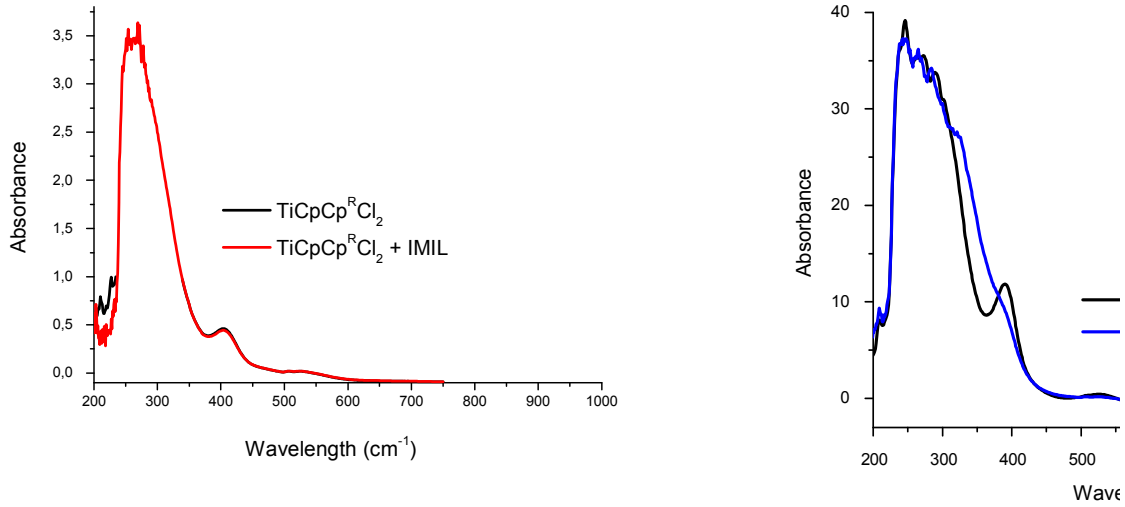

Figure S3. UV-Vis Spectra of $TiCpCp^RCl_2$, $TiCpCp^RCl_2$-IMIL, $TiCp_2Cl_2$ and $TiCp_2Cl_2$-IMIL in dichloromethane solution.

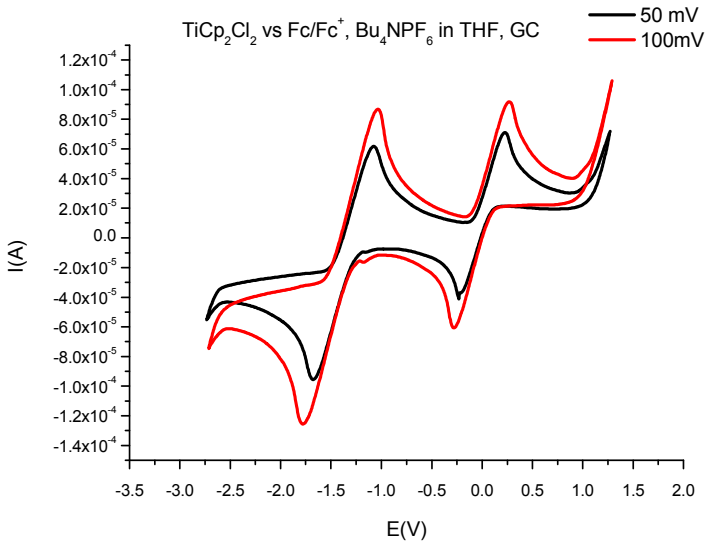

Figure S4. Cyclic voltammogram of $TiCp_2Cl_2$ scan rate 50 and 100 mV/s, in THF as solvent, Bu_4NPF_6 as electrolyte (0.2M), GC as working electrode, Pt as counter electrode and ferrocene/ferrocenium (Fc/Fc^+) couple as internal standard.

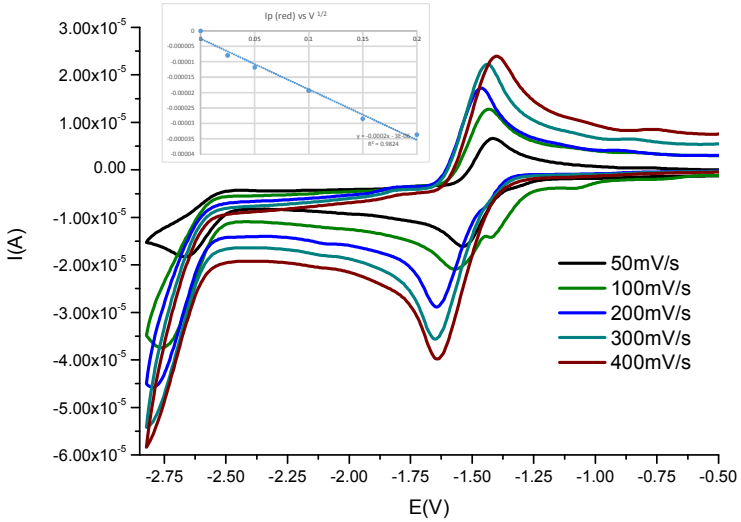

Figure S5. Figure Cyclic voltammogram of $TiCpCp^{R}Cl_2$ scan rate from 50-400 mV/s in THF as solvent, Bu_4NPF_6 as electrolyte (0.2M), GC as working electrode, Pt as counter electrode and Fc/Fc^{-} as internal standard.

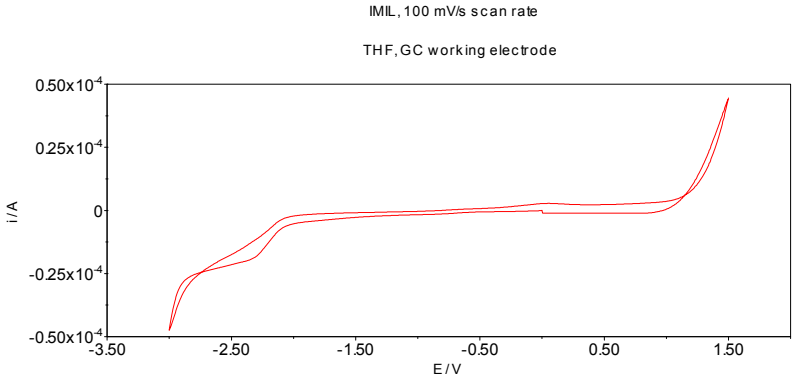

Figure S6. Cyclic voltammogram of IMIL scan rate 100 mV/s, in THF as solvent, Bu_4NPF_6 as electrolyte (0.2M), GC as working electrode, and Pt as counter electrode.

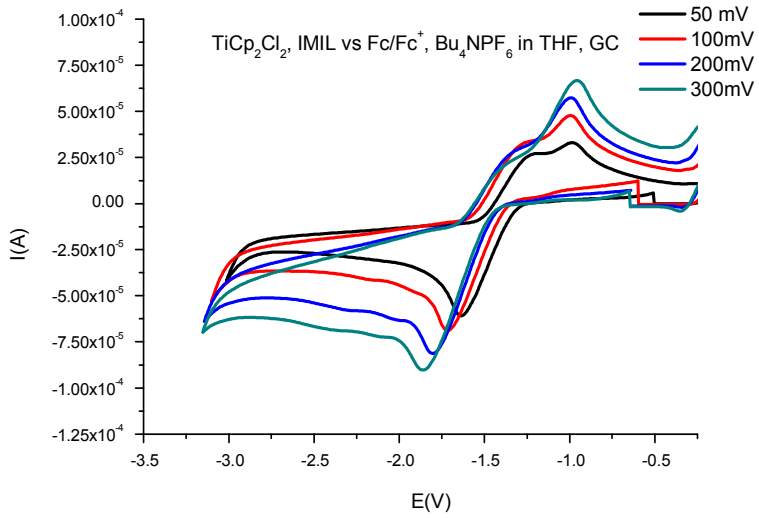

Figure S7. Cyclic voltammogram of $TiCp_2Cl_2$-IMIL scan rate from 50-100 mV/s, in THF as solvent, Bu_4NPF_6 as electrolyte (0.2M), GC as working electrode, Pt as counter electrode and Fc/Fc^+ as internal standard.

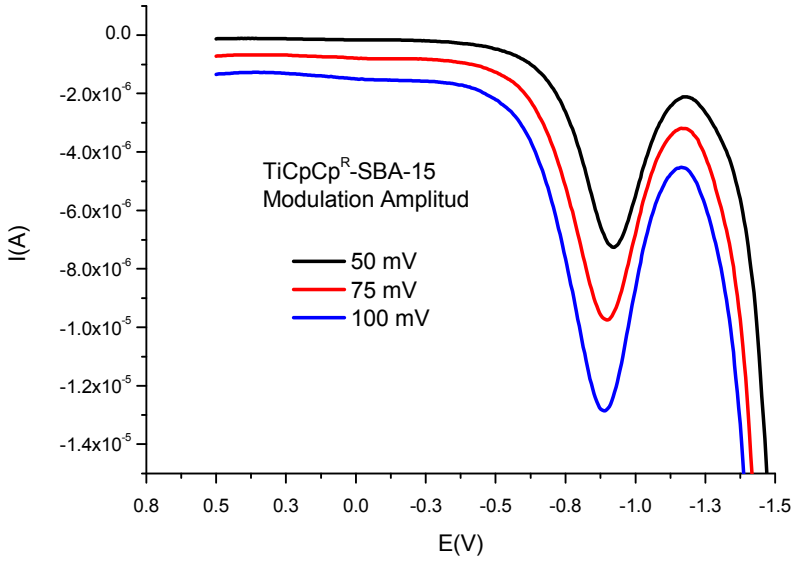

Figure S8. DPV of $TiCpCp^R$-SBA-15 immediately after immersion in aqueous phosphate buffer pH 7.4 as electrolyte at different values of modulation amplitude vs Ag/AgCl/KCl (3 M) as reference electrode.

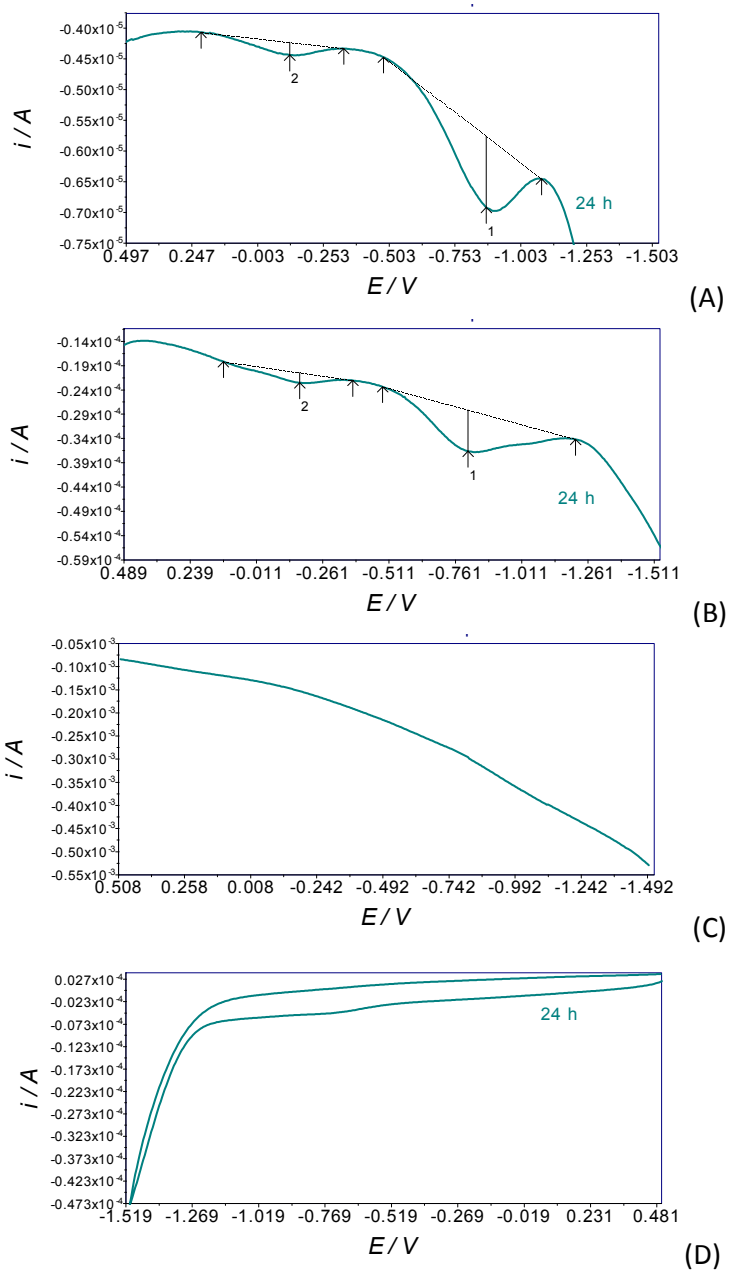

Figure S9. A) DPV of TiCpCp^{R}-SBA-15 24 h after immersion in aqueous phosphate buffer pH 7.4 as electrolyte. B) DPV of TiCpCp^{R}-SBA-15 24 h after immersion in freshly aqueous phosphate buffer pH 7.4 as electrolyte. C) and D) DPV and CV of aqueous phosphate buffer electrolyte used in (A) by using a commercial glassy carbon electrode as working electrode vs Ag/AgCl/KCl (3 M) as reference electrode.

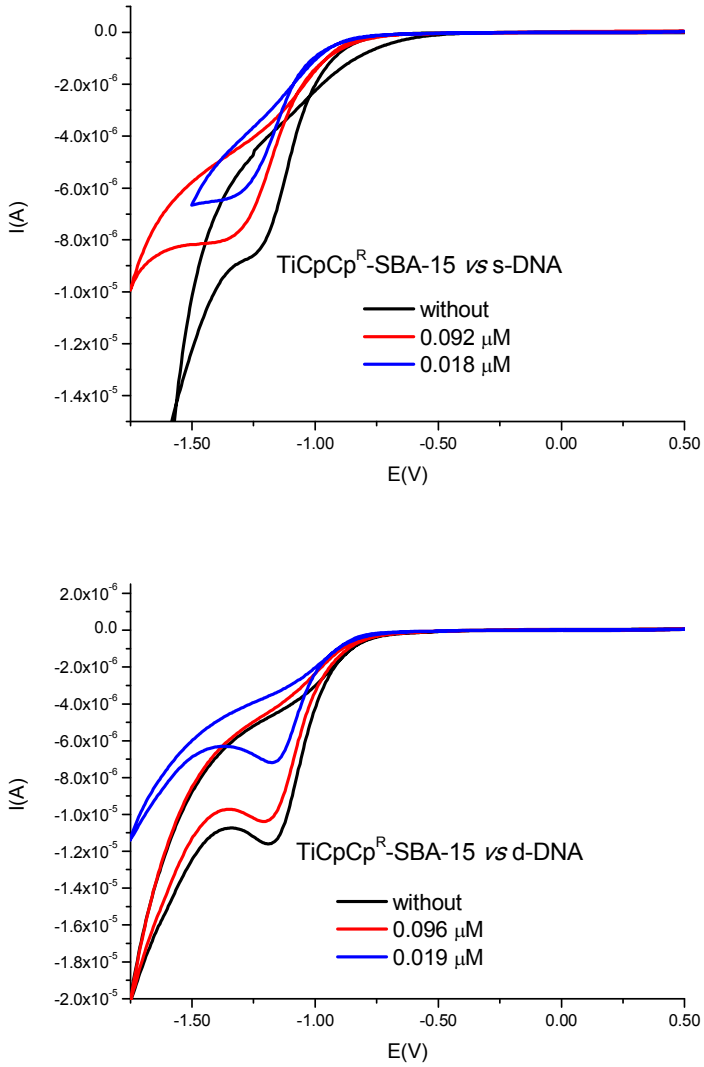

Figure S10. Cyclic voltammogram (100mV/s scan rate) of TiCpCp^{R}-SBA-15 vs single and double DNA 5 minutes after immersion and concentrations 0.092 and 0.018 mM in aqueous phosphate buffer pH 7.4 as electrolyte vs Ag/AgCl/KCl (3 M) as reference electrode.

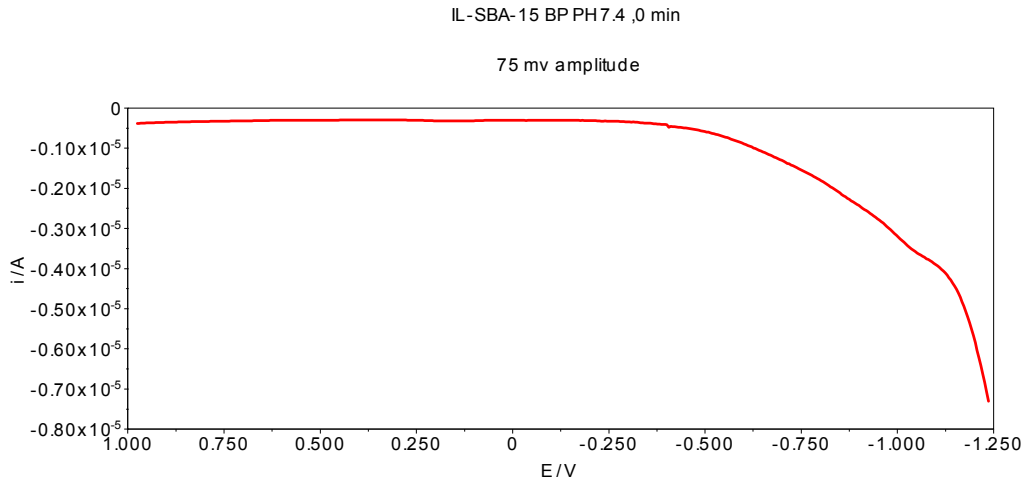

Figure S11. DPV of IMIL-SBA-15 after immersion in aqueous phosphate buffer pH 7.4 as electrolyte vs Ag/AgCl/KCl (3 M) as reference electrode.

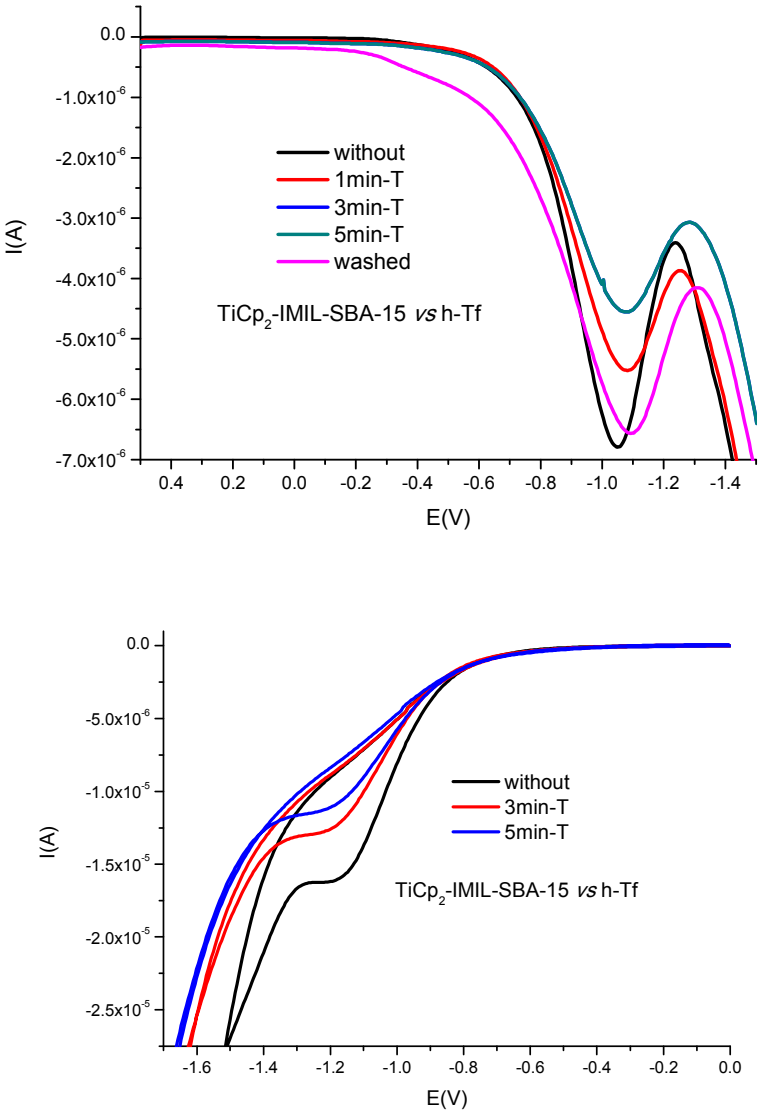

Figure S12. Differential pulse voltammograms (75 mV modulation amplitude) $TiCp_2$-IMIL-SBA-15 vs transferrin/graphite electrode after immersion into the aqueous transferrin as a function of time *vs* Ag/AgCl/KCl (3 M) as reference electrode.

1. D. Bradley, G. Williams, M, Lawton. *J. Org. Chem*. **2010**, *75*, 8351–8354.
2. D. Zhao, Q. Huo, J. Feng, B. F. Chmelka, G. D. Stucky, *J. Am. Chem. Soc.* **1998**, *120*, 6024–6036.
3. T. Sasaki, C. Zhong, M. Tada, Y. Iwasawa. *Chem. Commun.* **2005**, 2506–2508.